DOI: 10.1021/ic100438d

Inorganic Chemistry
Article

Pincer Phosphine Complexes of Ruthenium: Formation of Ru(P−O−P)(PPh_3)HCl (P−O−P = xantphos, DPEphos, $(Ph_2PCH_2CH_2)_2O$) and Ru(dppf)(PPh_3)HCl and Characterization of Cationic Dioxygen, Dihydrogen, Dinitrogen, and Arene Coordinated Phosphine Products

Araminta E. W. Ledger,[†] Aitor Moreno,[§] Charles E. Ellul,[‡] Mary F. Mahon,[‡] Paul S. Pregosin,[§] Michael K. Whittlesey,*[,†] and Jonathan M. J. Williams[†]

[†]*Department of Chemistry, and* [‡]*X-ray Crystallographic Unit, University of Bath, Claverton Down, Bath BA2 7AY, U.K., and* [§]*Laboratory of Inorganic Chemistry, ETHZ Hönggerberg CH-8093 Zurich, Switzerland*

Received March 5, 2010

Treatment of $Ru(PPh_3)_3HCl$ with the pincer phosphines 9,9-dimethyl-4,5-bis(diphenylphosphino)xanthene (xantphos), bis(2-diphenylphosphinophenyl)ether (DPEphos), or $(Ph_2PCH_2CH_2)_2O$ affords Ru(P−O−P)(PPh_3)HCl (xantphos, **1a**; DPEphos, **1b**; $(Ph_2PCH_2CH_2)_2O$, **1c**). The X-ray crystal structures of **1a**−**c** show that all three P−O−P ligands coordinate in a tridentate manner through phosphorus and oxygen. Abstraction of the chloride ligand from **1a**−**c** by $NaBAr_4^F$ (BAr_4^F = $B(3,5\text{-}C_6H_3(CF_3)_2)_4$) gives the cationic aqua complexes [Ru(P−O−P)(PPh_3)(H_2O)H]BAr_4^F (**3a**−**c**). Removal of chloride from **1a** by AgOTf yields Ru(xantphos)(PPh_3)H(OTf) (**2a**), which reacts with water to form [Ru(xantphos)(PPh_3)(H_2O)H](OTf). The aqua complexes **3a**−**b** react with O_2 to generate [Ru(xantphos)(PPh_3)(η^2-O_2)H]BAr_4^F (**5a**) and [Ru(DPEphos)(PPh_3)(η^2-O_2)H]BAr_4^F (**5b**). Addition of H_2 or N_2 to **3a**−**c** yields the thermally unstable dihydrogen and dinitrogen species [Ru(P−O−P)(PPh_3)(η^2-H_2)H]BAr_4^F (**6a**−**c**) and [Ru(P−O−P)(PPh_3)(N_2)H]BAr_4^F (**7a**−**c**), which have been characterized by multinuclear NMR spectroscopy at low temperature. $Ru(PPh_3)_3HCl$ reacts with 1,1′-bis(diphenylphosphino)ferrocene (dppf) to give the 16-electron complex Ru(dppf)(PPh_3)HCl (**1d**), which upon treatment with $NaBAr_4^F$, affords [Ru(dppf){(η^6-C_6H_5)PPh_2}H]BAr_4^F (**8**), in which the PPh_3 ligand binds η^6 through one of the PPh_3 phenyl rings. Reaction of **8** with CO or PMe_3 at elevated temperatures yields the 18-electron products [Ru(dppf)(PPh_3)$(CO)_2$H]$BAr^F{}_4$ (**9**) and [Ru$(PMe_3)_5$H]BAr_4^F (**10**).

Introduction

Tridentate phosphorus based pincer ligands containing two phosphines and a central linker group have become increasingly popular in recent years[1] for their ability to help stabilize unusual classes of ancillary ligands and less common metal oxidation states,[2] or afford metal complexes capable of either activating inert bonds[3] or bringing about novel catalytic transformations.[4] The most commonly encountered linker groups consist of either a metalated aryl ring in the anionic PCP or POCOP ligands (Chart 1) or a neutral donor such as a pyridine, which affords the general class of

*To whom correspondence should be addressed. E-mail: chsmkw@bath.ac.uk.

(1) (a) Albrecht, M.; van Koten, G. *Angew. Chem., Int. Ed.* **2001**, *40*, 3750–3781. (b) van der Boom, M. E.; Milstein, D. *Chem. Rev.* **2003**, *103*, 1759–1792. (c) Singleton, J. T. *Tetrahedron* **2003**, *59*, 1837–1857. (d) Benito-Garagorri, D.; Kirchner, K. *Acc. Chem. Res.* **2008**, *41*, 201–213.

(2) (a) Ashkenazi, N.; Vigalok, A.; Parthiban, S.; Ben-David, Y.; Shimon, L. J. W.; Martin, J. M. L.; Milstein, D. *J. Am. Chem. Soc.* **2000**, *122*, 8797–8798. (b) Conner, D.; Jayaprakash, K. N.; Cundari, T. R.; Gunnoe, T. B. *Organometallics* **2004**, *23*, 2724–2733. (c) Ingleson, M. J.; Pink, M.; Caulton, K. G. *J. Am. Chem. Soc.* **2006**, *128*, 4248–4249. (d) Pandarus, V.; Zargarian, D. *Chem. Commun.* **2007**, 978–980. (e) Ingleson, M. J.; Pink, M.; Fan, H.; Caulton, K. G. *J. Am. Chem. Soc.* **2008**, *130*, 4262–4276. (f) Hebden, T. J.; Denney, M. C.; Pons, V.; Piccoli, P. M. B.; Koetzle, T. F.; Schultz, A. J.; Kaminsky, W.; Goldberg, K. I.; Heinekey, D. M. *J. Am. Chem. Soc.* **2008**, *130*, 10812–10820. (g) van der Vlugt, J. I.; Pidko, E. A.; Vogt, D.; Lutz, M.; Spek, A. L.; Meetsma, A. *Inorg. Chem.* **2008**, *47*, 4442–4444. (h) Segawa, Y.; Yamashita, M.; Nozaki, K. *J. Am. Chem. Soc.* **2009**, *131*, 9201–9203.

(3) (a) Rybtchinski, B.; Vigalok, A.; Ben-David, Y.; Milstein, D. *J. Am. Chem. Soc.* **1996**, *118*, 12406–12415. (b) Dani, P.; Karlen, T.; Gossage, R. A.; Smeets, W. J. J.; Spek, A. L.; van Koten, G. *J. Am. Chem. Soc.* **1997**, *119*, 11317–11318. (c) van der Boom, M. E.; Liou, S.-Y.; Ben-David, Y.; Gozin, M.; Milstein, D. *J. Am. Chem. Soc.* **1998**, *120*, 13415–13421. (d) van der Boom, M. E.; Ben-David, Y.; Milstein, D. *J. Am. Chem. Soc.* **1999**, *121*, 6652–6656. (e) Dani, P.; Toorneman, M. A. M.; van Klink, G. P. M.; van Koten, G. *Organometallics* **2000**, *19*, 5287–5296. (f) Albrecht, M.; Dani, P.; Lutz, M.; Spek, A. L.; van Koten, G. *J. Am. Chem. Soc.* **2000**, *122*, 11822–11833. (g) Albrecht, M.; Spek, A. L.; Van Koten, G. *J. Am. Chem. Soc.* **2001**, *123*, 7233–7246. (h) Zhang, X.; Emge, T. J.; Ghosh, R.; Goldman, A. S. *J. Am. Chem. Soc.* **2005**, *127*, 8250–8251. (i) Ghosh, R.; Zhang, X.; Achord, P.; Emge, T. J.; Krogh-Jespersen, K.; Goldman, A. S. *J. Am. Chem. Soc.* **2007**, *129*, 853–866. (j) Prechtl, M. H. G.; Ben-David, Y.; Giunta, D.; Busch, S.; Taniguchi, Y.; Wisniewski, W.; Görls, H.; Mynott, R. J.; Theyssen, N.; Milstein, D.; Leitner, W. *Chem.—Eur. J.* **2007**, *13*, 1539–1546. (k) Bernskoetter, W. H.; Hanson, S. K.; Buzak, S. K.; Davis, Z.; White, P. S.; Swartz, R.; Goldberg, K. I.; Brookhart, M. *J. Am. Chem. Soc.* **2009**, *131*, 8603–8613.

Published on Web 06/24/2010

Chart 1

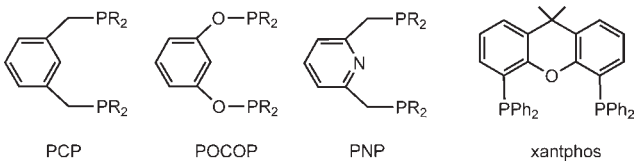

uncharged PNP ligands also shown in Chart 1. In the former group, the linker usually remains firmly coordinated to the metal center at all times, whereas in the latter case, temporary dissociation of either the linker or, alternatively, one of the phosphine arms can result in hemilabile behavior.

Neutral ligands based on a P−O−P motif are less common, despite the fact that the weak O→M interaction expected with a soft transition metal should make such ligands capable of both tridentate ("O in") and bidentate ("O out") coordination modes. The most well-known of the P−O−P systems are the xanthene based ligands, such as xantphos (Chart 1),[5] which in the vast majority of cases, coordinate in a bidentate ("O out") fashion. There are very few fully characterized examples of tridentate xanthene type ligands,[6−8] despite this binding mode being proposed to have relevance in a number of catalytic processes utilizing xantphos or other P−O−P type ligands.[9]

We have reported the use of Ru(xantphos)(PPh_3)(CO)H_2 and Ru(xantphos)(NHC)(CO)H_2 (NHC = N-heterocyclic carbene) in the "borrowing hydrogen" methodology for the activation of alcohols by reversible hydrogen transfer.[10] Both sets of compounds are coordinatively saturated, and consequently exhibit bidentate ("O out") coordination of the xantphos ligands. In efforts to further investigate the coordination chemistry of ruthenium xantphos and related P−O−P complexes,[8,11] we now describe the reactivity of the tridentate ("O in") cationic aqua species [Ru(P−O−P)(PPh_3)(H_2O)H]$^+$ (P−O−P = xantphos, DPEphos, ($Ph_2PCH_2CH_2$)$_2$O) with O_2, H_2, and N_2. The role played by oxygen coordination is highlighted by the different reactivity found with the bidentate ligand 1,1′-bis(diphenylphosphino)ferrocene (dppf).

Experimental Section

General Comments. All manipulations were carried out using standard Schlenk, high vacuum, and glovebox techniques. Solvents were purified using MBraun SPS and Innovative Technologies solvent systems (dichloromethane, toluene, tetrahydrofuran (THF)) or by distillation under argon from sodium benzophenone ketyl (benzene, hexane) or Mg/I_2 (ethanol). Deuterated solvents (Aldrich) were vacuum transferred from potassium (C_6D_6, THF-d_8) or calcium hydride (CD_2Cl_2). Literature methods (or slight variations of) were used for the preparation of Ru(PPh_3)$_3$HCl[12] and ($Ph_2PCH_2CH_2$)O.[7,13] Xantphos and DPEphos were purchased from Sigma-Aldrich and used as received. NMR spectra were recorded on Bruker Avance 400, 500, and 700 MHz spectrometers. ^{1}H and ^{13}C{^{1}H} spectra were referenced to the solvent as follows: δ 7.15 and δ 128.0 (C_6D_6); δ 5.32 and δ 53.7 (CD_2Cl_2); δ 3.58 and 25.4 (THF-d_8). ^{31}P{^{1}H} NMR chemical shifts were referenced externally to 85% H_3PO_4 (δ 0.0). ^{15}N shifts are given relative to nitromethane at δ = 0. Coupling constants for the spectra marked ^{31}P{^{1}H}* for **6b** and **7b** were determined by simulations performed using *g*-NMR.[14] IR spectra were recorded on a Nicolet Nexus FTIR spectrometer. Mass spectra were recorded using a microTOF electrospray time-of-flight (ESI-TOF) mass spectrometer (Bruker Daltonik GmbH) coupled to an Agilent 1200 LC system (Agilent Technologies). Elemental analyses were performed by Elemental Microanalysis Ltd., Okehampton, Devon, U.K. or the Elemental Analysis Service, London Metropolitan University, London, U.K.

Ru(xantphos)(PPh_3)HCl (1a). Ru(PPh_3)$_3$HCl (0.092 g, 0.1 mmol) and xantphos (0.069 g, 0.12 mmol) were refluxed together in dry THF (10 mL) for 3 h to give a bright orange solution. After removal of the solvent, the product was washed in hexane (3 × 10 mL) and recrystallized from benzene/hexane to give orange needle-like crystals (0.086 g, 88%). Selected ^{1}H NMR (C_6D_6, 400 MHz, 298 K): δ −16.22 (dt, $^2J_{HP}$ = 27.2 Hz, $^2J_{HP}$ = 23.9 Hz, 1H, RuH), 1.25 (s, 3H, C(CH_3)$_2$), 1.30 (s, 3H, C(CH_3)$_2$). ^{31}P{^{1}H} (C_6D_6, 162 MHz, 298 K): δ 75.2 (t, $^2J_{PP}$ = 33 Hz), 46.7 (d, $^2J_{PP}$ = 33 Hz). Anal. Calcd (%) for $C_{57}H_{48}OP_3ClRu \cdot 2C_6H_6$ (1134.66): C 73.04, H 5.33; found: C 72.63, H 5.41.

Ru(DPEphos)(PPh_3)HCl (1b). As for **1a** by refluxing Ru(PPh_3)$_3$HCl (0.092 g, 0.1 mmol) and DPEphos (0.162 g, 0.3 mmol)

(4) (a) Gupta, M.; Hagen, C.; Kaska, W. C.; Cramer, R. E.; Jensen, C. M. *J. Am. Chem. Soc.* **1997**, *119*, 840–841. (b) Jensen, C. M. *Chem. Commun.* **1999**, 2443–2449. (c) Göttker-Schnetmann, I.; White, P. S.; Brookhart, M. *J. Am. Chem. Soc.* **2004**, *2004*, 1804–1811. (d) Fan, L.; Ozerov, O. V. *Chem. Commun.* **2005**, 4450–4452. (e) Zhang, J.; Leitus, G.; Ben-David, Y.; Milstein, D. *Angew. Chem., Int. Ed.* **2006**, *45*, 1113–1115. (f) Goldman, A. S.; Roy, A. H.; Huang, Z.; Ahuja, R.; Schinski, W.; Brookhart, M. *Science* **2006**, *312*, 257–261. (g) Gunanathan, C.; Shimon, L. J. W.; Milstein, D. *J. Am. Chem. Soc.* **2009**, *131*, 3146–3147.

(5) For reviews, see: (a) Dierkes, P.; van Leeuwen, P. W. N. M. *J. Chem. Soc., Dalton Trans.* **1999**, 1519–1530. (b) van Leeuwen, P. W. N. M.; Kamer, P. C. J.; Reek, J. N. H.; Dierkes, P. *Chem. Rev.* **2000**, *100*, 2741–2769. (c) Kamer, P. C. J.; van Leeuwen, P. W. N. M.; Reek, J. N. H. *Acc. Chem. Res.* **2001**, *34*, 895–904. (d) Freixa, Z.; van Leeuwen, P. W. N. M. *Dalton Trans.* **2003**, 1890–1901. (e) Birkholz (née Gensow), M.-N.; Freixa, Z.; van Leeuwen, P. W. N. M. *Chem. Soc. Rev.* **2009**, *38*, 1099–1118.

(6) (a) Alcock, N. W.; Brown, J. M.; Jeffery, J. C. *J. Chem. Soc., Dalton Trans.* **1976**, 583–588. (b) Steffey, B. D.; Miedaner, A.; Maciejewski-Farmer, M. L.; Berantis, P. R.; Herring, A. M.; Allured, V. S.; Carperos, V.; DuBois, D. L. *Organometallics* **1994**, *13*, 4844–4855. (c) Kataoka, Y.; Tsuji, Y.; Matsumoto, O.; Ohashi, M.; Yamagata, T.; Tani, K. *J. Chem. Soc., Chem. Commun.* **1995**, 2099–2100. (d) Moxham, G. L.; Randell-Sly, H.; Brayshaw, S. K.; Weller, A. S.; Willis, M. C. *Chem.—Eur. J.* **2008**, *14*, 8383–8397.

(7) Bolzati, C.; Boschi, A.; Uccelli, L.; Tisato, F.; Refosco, F.; Cagnolini, A.; Duatti, A.; Prakash, S.; Bandolini, G.; Vittadini, A. *J. Am. Chem. Soc.* **2002**, *124*, 11468–11479.

(8) Major, Q.; Lough, A. J.; Gusev, D. G. *Organometallics* **2005**, *24*, 2492–2501.

(9) (a) Moxham, G. L.; Randell-Sly, H.; Brayshaw, S. K.; Woodward, R. L.; Weller, A. S.; Willis, M. C. *Angew. Chem., Int. Ed.* **2006**, *45*, 7618–7622. (b) Ohshima, T.; Miyamoto, Y.; Ipposhi, J.; Nakahara, Y.; Utsunomiya, M.; Mashima, K. *J. Am. Chem. Soc.* **2009**, *131*, 14317–14328.

(10) (a) Slatford, P. A.; Whittlesey, M. K.; Williams, J. M. J. *Tetrahedron Lett.* **2006**, *47*, 6787–6789. (b) Pridmore, S. J.; Slatford, P. A.; Williams, J. M. J. *Tetrahedron Lett.* **2007**, *48*, 5111–5114. (c) Anand, N.; Owston, N. A.; Parker, A. J.; Slatford, P. A.; Williams, J. M. J. *Tetrahedron Lett.* **2007**, *48*, 7761–7763. (d) Pridmore, S. J.; Slatford, P. A.; Taylor, J. E.; Whittlesey, M. K.; Williams, J. M. J. *Tetrahedron* **2009**, *65*, 8981–8986. (e) Owston, N. A.; Nixon, T. D.; Parker, A. J.; Whittlesey, M. K.; Williams, J. M. J. *Synthesis* **2009**, 1578–1581. (f) Ledger, A. E. W.; Slatford, P. A.; Lowe, J. P.; Mahon, M. F.; Whittlesey, M. K.; Williams, J. M. J. *Dalton Trans.* **2009**, 716–722. (g) Ledger, A. E. W.; Mahon, M. F.; Whittlesey, M. K.; Williams, J. M. J. *Dalton Trans.* **2009**, 6941–6947.

(11) (a) Kranenburg, M.; Kamer, P. C. J.; van Leeuwen, P. W. N. M.; Chaudret, B. *Chem. Commun.* **1997**, 373–374. (b) Lenero, K. A.; Kranenburg, M.; Guari, Y.; Kamer, P. C. J.; van Leeuwen, P. W. N. M.; Sabo-Etienne, S.; Chaudret, B. *Inorg. Chem.* **2003**, *42*, 2859–2866. (c) van Engelen, M. C.; Teunissen, H. T.; de Vries, J. G.; Elsevier, C. J. *J. Mol. Catal. A* **2003**, *206*, 185–192. (d) Deb, B.; Dutta, D. K. *Polyhedron* **2009**, *28*, 2258–2262. (e) Deb, B.; Borah, B. J.; Sarmah, B. J.; Das, B.; Dutta, D. K. *Inorg. Chem. Commun.* **2009**, *12*, 868–871.

(12) Schunn, R. A.; Wonchoba, E. R.; Wilkinson, G. *Inorg. Synth.* **1971**, *13*, 131–134.

(13) (a) Sacconi, L.; Gelsomini, J. *Inorg. Chem.* **1968**, *7*, 291–294. (b) Thewissen, D. H. M. W.; Timmer, K.; Noltes, J. G.; Marsman, J. W.; Laine, R. M. *Inorg. Chim. Acta* **1985**, *97*, 143–150.

(14) Budzelaar, P. H. M. *g-NMR*, version 4; Cherwell Scientific Publishing Ltd: Oxford, 1994−1997.

in THF for 1.5 h. After washing with hexane, recrystallization from CH_2Cl_2/hexane gave orange needle-like crystals of the product in 65% yield (0.061 g). Selected ^{1}H NMR (CD_2Cl_2, 400 MHz, 298 K): δ −16.34 (dt, $^2J_{HP}$ = 27.6 Hz, $^2J_{HP}$ = 23.6 Hz, 1H, RuH). $^{31}P\{^1H\}$ (CD_2Cl_2, 162 MHz, 298 K): δ 75.3 (t, $^2J_{PP}$ = 30.9 Hz), 46.7 (br s). $^{31}P\{^1H\}$ (CD_2Cl_2, 162 MHz, 233 K): δ 75.0 (t, $^2J_{PP}$ = 31 Hz), 39.7 (dd, $^2J_{PP}$ = 285 Hz, $^2J_{PP}$ = 31 Hz), 30.8 (dd, $^2J_{PP}$ = 285 Hz, $^2J_{PP}$ = 31 Hz). Anal. Calcd (%) for $C_{54}H_{44}OP_3ClRu\cdot0.5CH_2Cl_2$ (885.79): C 66.74, H 4.62; found: C 66.77, H 4.82.

Ru((Ph$_2$PCH$_2$CH$_2$)$_2$O)(PPh$_3$)HCl (1c). As for **1a** by refluxing $Ru(PPh_3)_3HCl$ (0.092 g, 0.1 mmol) and $(Ph_2PCH_2CH_2)_2O$ (0.049 g, 0.12 mmol) in THF for 0.5 h. After hexane washing, recrystallization from CH_2Cl_2/hexane gave orange crystals of the product in 60% yield (0.051 g). Selected ^{1}H NMR (CD_2Cl_2, 500 MHz, 298 K): δ −17.54 (dt, $^2J_{HP}$ = 28.5 Hz, $^2J_{HP}$ = 21.7 Hz, 1H, RuH), 2.48 (m, 2H, PCH_2), 2.72 (m, 2H, PCH_2), 3.37 (m, 2H, OCH_2), 4.11 (m, 2H, OCH_2). $^{31}P\{^1H\}$ (CD_2Cl_2, 202 MHz, 298 K): δ 71.0 (t, $^2J_{PP}$ = 32 Hz), 42.3 (d, $^2J_{PP}$ = 32 Hz). Anal. Calcd (%) for $C_{46}H_{44}OP_3ClRu\cdot0.75CH_2Cl_2$ (906.00): C 61.98, H 5.06; found: C 61.98, H 5.24.

Ru(xantphos)(PPh$_3$)H(OTf) (2a). A CH_2Cl_2 solution (10 mL) of **1a** (0.200 g, 0.20 mmol) and AgOTf (0.086 g, 0.22 mmol) was stirred in an ampule fitted with a J. Young's PTFE tap at room temperature for 15 h and then filtered to remove a gray precipitate of AgCl. The solvent was reduced by half and layered with hexane to afford yellow crystals of **2a** (0.132 g, 59%). Selected ^{1}H NMR (CD_2Cl_2, 400 MHz, 315 K): δ −22.27 (dt, $^2J_{HP}$ = 31.0 Hz, $^2J_{HP}$ = 22.6 Hz, 1H, RuH). $^{31}P\{^1H\}$ (CD_2Cl_2, 162 MHz, 315 K): δ 68.9 (t, $^2J_{PP}$ = 31 Hz), 44.9 (d, $^2J_{PP}$ = 31 Hz). ^{19}F NMR (CD_2Cl_2, 376 MHz, 298 K): δ −78.8 (s, OTf). Anal. Calcd (%) for $C_{58}H_{48}O_4P_3SF_3Ru$ (1092.07): C 63.79, H 4.43; found: C 63.66, H 4.30.

[Ru(xantphos)(PPh$_3$)(H$_2$O)H]BAr$_4^F$ (3a). A CD_2Cl_2 solution of **1a** (0.010 g, 0.01 mmol) and $NaBAr_4^F$ (0.009 g, 0.011 mmol) was left to stand in an NMR tube fitted with a resealable J. Young's PTFE valve at room temperature for 15 h to afford the product. Selected ^{1}H NMR (CD_2Cl_2, 400 MHz, 298 K): δ −19.67 (dt, $^2J_{HP}$ = 29.4 Hz, $^2J_{HP}$ = 18.6 Hz, 1H, RuH). $^{31}P\{^1H\}$ (CD_2Cl_2, 162 MHz, 298 K): δ 73.2 (t, $^2J_{PP}$ = 28 Hz), 46.9 (d, $^2J_{PP}$ = 28 Hz). ESI-TOF MS: $[M\text{-}H_2O]^+$ m/z = 943.1993 (theoretical 943.1972).

The corresponding triflate salt [Ru(xantphos)(PPh$_3$)(H$_2$O)H]OTf was prepared by stirring **1a** (0.098 g, 0.10 mmol) with AgOTf (0.043 g, 0.11 mmol) in CH_2Cl_2 (10 mL) for 15 h. After filtration to remove AgCl, degassed H_2O (0.027 mL, 0.001 mol) was added and the suspension stirred for 30 min. The volume of solvent was reduced by half and a layer of hexane added. This afforded yellow crystals, at least some of which corresponded to [Ru(xantphos)(PPh$_3$)(H$_2$O)H]OTf on the basis of X-ray diffraction.[15] NMR analysis of the crystalline material as a whole showed it to consist of both the aqua complex (0.045 g, 41%) and [Ru(xantphos)(PPh$_3$)(η^2-O$_2$)H]OTf (0.011 g, 10%). The latter species was always formed as a side product in varying amounts, and could not be separated. This excluded the possibility of determining CHN analysis of the aqua complex.

[Ru(DPEphos)(PPh$_3$)(H$_2$O)H]BAr$_4^F$ (3b). As for **3a**, but with **1b** (0.009 g, 0.01 mmol) and $NaBAr_4^F$ (0.009 g, 0.011 mmol). Selected ^{1}H NMR (CD_2Cl_2, 400 MHz, 298 K): δ −18.67 (dt, $^2J_{HP}$ = 31.4 Hz, $^2J_{HP}$ = 20.2 Hz, 1H, RuH). $^{31}P\{^1H\}$ (CD_2Cl_2, 162 MHz, 298 K): δ 72.0 (br s), 45.1 (br s).

[Ru((Ph$_2$PCH$_2$CH$_2$)$_2$O)(PPh$_3$)(H$_2$O)H]BAr$_4^F$ (3c). As for **3a**, but with **1c** (0.008 g, 0.01 mmol) and $NaBAr_4^F$ (0.009 g, 0.011). Selected ^{1}H NMR (CD_2Cl_2, 400 MHz, 298 K): δ −21.05 (dt, $^2J_{HP}$ = 30.3 Hz, $^2J_{HP}$ = 18.1 Hz, 1H, RuH). $^{31}P\{^1H\}$ (CD_2Cl_2, 162 MHz, 298 K): δ 72.4.2 (t, $^2J_{PP}$ = 29 Hz), 47.8 (d, $^2J_{PP}$ = 29 Hz).

(15) The X-ray structure of this complex is provided in the Supporting Information.

[Ru(xantphos)(PPh$_3$)(MeCN)H]BAr$^F_4$ (4a). A CD_2Cl_2 solution of **1a** (0.010 g, 0.01 mmol) and $NaBAr_4^F$ (0.009 g, 0.011 mmol) was left to stand in an NMR tube fitted with a resealable J. Young's PTFE valve at room temperature for 15 h. MeCN (0.003 mL, 0.05 mmol) was then added to the solution via syringe. The product, [Ru(xantphos)(PPh$_3$)(MeCN)H]BAr$^F_4$ (**4a**), was spectroscopically characterized. Selected ^{1}H NMR (CD_2Cl_2, 500 MHz, 298 K): δ −13.39 (dt, $^2J_{HP}$ = 27.0 Hz, $^2J_{HP}$ = 19.1 Hz, 1H, RuH), 1.36 (s, 3H, NC−CH_3). $^{31}P\{^1H\}$ (CD_2Cl_2, 202 MHz, 298 K): δ 75.8 (br), 51.2 (d, $^2J_{PP}$ = 30 Hz). Selected $^{13}C\{^1H\}$ NMR (CD_2Cl_2, 126 MHz, 298 K): δ 2.9 (s, NC-*C*H$_3$), 121.8 (s, N*C*-CH$_3$). IR (nujol, cm^{-1}): 2241 (ν_{CN}). Comparable spectroscopic data was recorded for the corresponding triflate salt, which was prepared by addition of MeCN (0.003 mL, 0.05 mmol) to a CD_2Cl_2 solution of **2a** (0.011 g, 0.01 mmol) in a J. Youngs NMR tube. Selected ^{1}H NMR (CD_2Cl_2, 500 MHz, 298 K): δ −13.42 (dt, $^2J_{HP}$ = 27.0 Hz, $^2J_{HP}$ = 19.1 Hz, 1H, RuH), 1.42 (s, 3H, NC−CH_3). $^{31}P\{^1H\}$ (CD_2Cl_2, 202 MHz, 298 K): δ 76.1 (br), 51.4 (d, $^2J_{PP}$ = 30 Hz).

[Ru(xantphos)(PPh$_3$)(η^2-O$_2$)H]BAr$_4^F$ (5a). A CH_2Cl_2 solution (10 mL) of **1a** (0.120 g, 0.12 mmol) and $NaBAr_4^F$ (0.110 g, 0.14 mmol) was stirred in an ampule fitted with a J. Young's PTFE tap at room temperature for 15 h and then filtered to remove the white precipitate of NaCl. The filtrate was opened to air and left stirring for 10 min, before the solvent was removed in vacuo. The resulting solid was washed with hexane (10 mL) and recrystallized from CH_2Cl_2/hexane to afford brown crystals of **5a** (0.109 g, 49%). Selected ^{1}H NMR (CD_2Cl_2, 400 MHz, 298 K): δ −1.48 (dt, $^2J_{HP}$ = 29.4 Hz, $^2J_{HP}$ = 27.2 Hz, 1H, RuH), 1.45 (s, 3H, $C(CH_3)_2$), 1.87 (s, 3H, $C(CH_3)_2$). $^{31}P\{^1H\}$ (CD_2Cl_2, 162 MHz, 298 K): δ 48.2 (t, $^2J_{PP}$ = 19 Hz), 44.4 (d, $^2J_{PP}$ = 19 Hz). Anal. Calcd (%) for $C_{89}H_{60}BO_3F_{24}P_3Ru$ (1838.17): C 58.15, H 3.29; found: C 57.98, H 3.10. ESI-TOF MS: $[M]^+$ m/z = 975.1931 (theoretical 975.1870).

[Ru(DPEphos)(PPh$_3$)(η^2-O$_2$)H]BAr$_4^F$ (5b). As for **5a** using **1b** (0.100 g, 0.11 mmol) and $NaBAr_4^F$ (0.095 g, 0.12 mmol). After exposure to air and removal of the solvent, the resulting solid was washed twice with hexane (10 mL) and sonicated before being dried overnight under vacuum to give **5b** as a tan solid (0.090 g, 48%). Larger scale recrystallization proved difficult because of facile overoxidation of the complex in solution. Selected ^{1}H NMR (CD_2Cl_2, 400 MHz, 298 K): δ −2.01 (dt, $^2J_{HP}$ = 32.0 Hz, $^2J_{HP}$ = 30.4 Hz, 1H, RuH). $^{31}P\{^1H\}$ (CD_2Cl_2, 162 MHz, 298 K): δ 41.4 (t, $^2J_{PP}$ = 19 Hz), 36.2 (d, $^2J_{PP}$ = 19 Hz). ESI-TOF MS: $[M]^+$ m/z = 935.1600 (theoretical 935.1556).

[Ru((Ph$_2$PCH$_2$CH$_2$)$_2$O)(PPh$_3$)(η^2-O$_2$)H]BAr$_4^F$ (5c). A CD_2Cl_2 solution of **1c** (0.008 g, 0.01 mmol) and $NaBAr_4^F$ (0.009 g, 0.011) in a resealable J. Young's NMR tube was prepared at room temperature, and after being left for 15 h, exposed to air, which resulted in an rapid color change from yellow to yellow-green. NMR spectra of [Ru((Ph$_2$PCH$_2$CH$_2$)$_2$O)(PPh$_3$)(η^2-O$_2$)H]BAr$_4^F$ (**5c**) were run immediately to minimize the degradation of the complex. Selected ^{1}H NMR (CD_2Cl_2, 400 MHz, 298 K): δ −2.88 (dt, $^2J_{HP}$ = 29.6 Hz, $^2J_{HP}$ = 25.9 Hz, 1H, RuH), 2.42−2.61 (m, 4H, PCH_2), 3.48 (m, 2H, OCH_2), 3.74 (m, 2H, OCH_2). $^{31}P\{^1H\}$ (CD_2Cl_2, 162 MHz, 298 K): δ 48.2 (t, $^2J_{PP}$ = 19 Hz), 45.8 (d, $^2J_{PP}$ = 19 Hz).

[Ru(xantphos)(PPh$_3$)(η^2-H$_2$)H]BAr$_4^F$ (6a). A CD_2Cl_2 solution of **1a** (0.010 g, 0.01 mmol) and $NaBAr_4^F$ (0.009 g, 0.011 mmol) was left to stand in an NMR tube fitted with a resealable J. Young's PTFE valve at room temperature for 15 h. The solution was freeze−pump−thaw degassed three times and placed under 1 atm of H_2 to give a mixture of [Ru(xantphos)(PPh$_3$)(η^2-H$_2$)H]BAr$_4^F$ (**6a**) and unreacted **3a** in a ratio of 3.1:1 at 180 K. Selected ^{1}H NMR (CD_2Cl_2, 400 MHz, 180 K): δ −8.79 (dt, $^2J_{HP}$ = 22.4 Hz, $^2J_{HP}$ = 19.1 Hz, 1H, RuH), −0.95 (broad s, 2H, η^2-H$_2$), 1.42 (s, 3H, $C(CH_3)_2$), 1.61 (s, 3H, $C(CH_3)_2$). $^{31}P\{^1H\}$ (CD_2Cl_2, 162 MHz, 180 K): δ 67.6 (t, $^2J_{PP}$ = 28 Hz), 51.9 (d, $^2J_{PP}$ = 28 Hz).

[Ru(DPEphos)(PPh$_3$)(η^2-H$_2$)H]BAr$_4^F$ (6b). As for **6a**, but with **1b** (0.009 g, 0.01 mmol) and NaBAr$_4^F$ (0.009 g, 0.011 mmol) to afford a mixture of [Ru(DPEphos)(PPh$_3$)(η^2-H$_2$)H]BAr$_4^F$ (**6b**) and **3b** in a ratio of 6.1:1 at 195 K. Selected ^{1}H NMR (CD_2Cl_2, 400 MHz, 195 K): δ −7.95 (dt, $^2J_{HP}$ = 22.8 Hz, $^2J_{HP}$ = 19.4 Hz, 1H, RuH), −0.25 (broad s, 2H, η^2-H$_2$). ^{31}P{^{1}H}* (CD_2Cl_2, 162 MHz, 195 K): δ 69.2 (t, $^2J_{PP}$ = 26 Hz), 47.1 (dd, $^2J_{PP}$ = 226 Hz, $^2J_{PP}$ = 26 Hz), 46.2 (dd, $^2J_{PP}$ = 226 Hz, $^2J_{PP}$ = 26 Hz).

[Ru((Ph$_2$PCH$_2$CH$_2$)$_2$O)(PPh$_3$)(η^2-H$_2$)H]BAr$_4^F$ (6c). As for **6a**, but with **1c** (0.008 g, 0.01 mmol) and NaBAr$_4^F$ (0.009 g, 0.011 mmol) to afford a mixture of [Ru((Ph$_2$PCH$_2$CH$_2$)$_2$O)(PPh$_3$)(η^2-H$_2$)H]BAr$_4^F$ (**6c**) and unreacted **3c** in a ratio of 4.4:1 at 195 K. Selected ^{1}H NMR (CD_2Cl_2, 400 MHz, 195 K): δ −9.16 (dt, $^2J_{HP}$ = 23.6 Hz, $^2J_{HP}$ = 16.2 Hz, 1H, RuH), −1.91 (broad s, 2H, η^2-H$_2$), 2.35 (m, 2H, PCH$_2$), 2.60 (m, 2H, PCH$_2$), 3.17 (m, 2H, OCH$_2$), 3.71 (m, 2H, OCH$_2$). ^{31}P{^{1}H} (CD_2Cl_2, 162 MHz, 195 K): δ 66.9 (t, $^2J_{PP}$ = 27 Hz), 56.2 (d, $^2J_{PP}$ = 27 Hz).

[Ru(xantphos)(PPh$_3$)(N$_2$)H]BAr$_4^F$ (7a). A CD_2Cl_2 solution of **1a** (0.010 g, 0.01 mmol) and NaBAr$_4^F$ (0.009 g, 0.011 mmol) was left to stand in an NMR tube fitted with a resealable J. Young's PTFE valve at room temperature for 15 h. The solution was freeze−pump−thaw degassed three times and placed under 1 atm of N_2 to give a mixture of [Ru(xantphos)(PPh$_3$)(N$_2$)H]BAr$_4^F$ (**7a**) and unreacted **3a** in a ratio of 6.7:1 at 180 K. Selected ^{1}H NMR (CD_2Cl_2, 400 MHz, 180 K): δ −11.72 (dt, $^2J_{HP}$ = 26.0 Hz, $^2J_{HP}$ = 16.5 Hz, 1H, RuH: ^{1}H{^{31}P} NMR spectrum recorded with ^{15}N labeling: δ −11.76 (d, $^2J_{HN}$ = 17.9 Hz)), 1.46 (s, 3H, C(CH$_3$)$_2$), 1.66 (s, 3H, C(CH$_3$)$_2$). ^{31}P{^{1}H} (CD_2Cl_2, 162 MHz, 180 K): δ 68.2 (t, $^2J_{PP}$ = 27 Hz), 47.8 (d, $^2J_{PP}$ = 27 Hz). ^{15}N{^{1}H} (CD_2Cl_2, 400 MHz, 180 K): δ −88.7 (s, α-N), −57.6 (s, β-N).

[Ru(DPEphos)(PPh$_3$)(N$_2$)H]BAr$_4^F$ (7b). As for **7a**, but with **1b** (0.009 g, 0.01 mmol) and NaBAr$_4^F$ (0.009 g, 0.011 mmol) to give a mixture of [Ru(DPEphos)(PPh$_3$)(N$_2$)H]BAr$_4^F$ (**7b**) and unreacted **3b** in a ratio of 4.5:1 at 180 K. Selected ^{1}H NMR (CD_2Cl_2, 400 MHz, 180 K): δ −11.04 (dt, $^2J_{HP}$ = 26.7 Hz, $^2J_{HP}$ = 20.0 Hz, 1H, RuH: ^{1}H{^{31}P} NMR spectrum recorded with ^{15}N labeling: δ −11.06 (d, $^2J_{HN}$ = 16.9 Hz)). ^{31}P{^{1}H}* (CD_2Cl_2, 162 MHz, 180 K): δ 65.4 (t, $^2J_{PP}$ = 27 Hz), 43.1 (dd, $^2J_{PP}$ = 241 Hz, $^2J_{PP}$ = 25 Hz), 41.7 (dd, $^2J_{PP}$ = 241 Hz, $^2J_{PP}$ = 28 Hz). ^{15}N{^{1}H} (CD_2Cl_2, 400 MHz, 180 K): δ −82.6 (s, α-N), −51.8 (s, β-N).

[Ru((Ph$_2$PCH$_2$CH$_2$)$_2$O)(PPh$_3$)(N$_2$)H]BAr$_4^F$ (7c). As for **7a**, but with **1c** (0.008 g, 0.01 mmol) and NaBAr$_4^F$ (0.009 g, 0.011 mmol) to afford a mixture of [Ru((Ph$_2$PCH$_2$CH$_2$)$_2$O)(PPh$_3$)(N$_2$)H]BAr$_4^F$ (**7c**) and unreacted **3c** in a ratio of 2.4:1 at 195 K. Selected ^{1}H NMR (CD_2Cl_2, 400 MHz, 195 K): δ −12.06 (dt, $^2J_{HP}$ = 25.3 Hz, $^2J_{HP}$ = 16.6 Hz, 1H, RuH: ^{1}H{^{31}P} NMR spectrum recorded with ^{15}N labeling: δ −12.08 (d, $^2J_{HN}$ = 18.1 Hz)), 2.11 (m, 2H, P−C*H*H), 2.70 (m, 2H, P-CH*H*), 3.28 (m, 2H, O−C*H*H), 3.87 (m, 2H, O−CH*H*). ^{31}P{^{1}H} (CD_2Cl_2, 162 MHz, 195 K): δ 67.2 (t, $^2J_{PP}$ = 27 Hz), 51.1 (d, $^2J_{PP}$ = 27 Hz). ^{15}N{^{1}H} (CD_2Cl_2, 400 MHz, 195 K): δ −86.2 (s, α-N), −59.1 (s, β-N).

Ru(dppf)(PPh$_3$)HCl (1d). As for **1a** by refluxing Ru(PPh$_3$)$_3$HCl (0.092 g, 0.1 mmol) and dppf (0.055 g, 0.12 mmol) in THF (10 mL) for 0.5 h. After hexane washing, recrystallization from THF/hexane gave orange crystals of the product in 48% yield (0.046 g). Selected ^{1}H NMR (THF-d_8, 500 MHz, 298 K): δ −19.99 (dt, $^2J_{HP}$ = 29.9 Hz, $^2J_{HP}$ = 19.9 Hz, 1H, RuH), 4.16 (s, 2H, C_5H_4), 4.27 (s, 2H, C_5H_4), 4.30 (s, 2H, C_5H_4), 4.51 (s, 2H, C_5H_4). ^{31}P{^{1}H} (THF-d_8, 162 MHz, 298 K): δ 64.9 (br s), 41.4 (t, $^2J_{PP}$ = 134 Hz). 213 K: δ 83.1 (br s), 48.4 (dd, $^2J_{PP}$ = 299 Hz, $^2J_{PP}$ = 30 Hz), 41.5 (dd, $^2J_{PP}$ = 294 Hz, $^2J_{PP}$ = 25 Hz). Anal. Calcd (%) for $C_{52}H_{44}P_3ClFeRu\cdot 3C_4H_8O$ (1170.54): C 65.67, H 5.86; found: C 65.56, H 6.11.

[Ru(dppf)({η^6-C$_6$H$_5$}PPh$_2$)H]BAr$_4^F$ (8). Complex **1d** (0.095 g, 0.10 mmol) and NaBAr$^F_4$ (0.089 g, 0.11 mmol) were charged to an ampule fitted with a J. Young's PTFE tap, dissolved in CH_2Cl_2 (10 mL) and stirred at room temperature for 15 h. The suspension was filtered by cannula to remove NaCl, and the filtrate reduced to dryness. The resulting orange solid was washed with hexane (2 × 10 mL) and recrystallized from CH_2Cl_2/hexane (Yield: 0.178 g, 52%). Selected ^{1}H NMR (CD_2Cl_2, 400 MHz, 298 K): δ −9.32 (dt, $^2J_{HP}$ = 38.8 Hz, J_{HP} = 7.0 Hz, 1H, RuH), 4.20 (m, 2H, C_5H_4), 4.32 (m, 2H, C_5H_4), 4.36 (m, 4H, C_5H_4), 4.72 (m, 2H, η^6-$C_6H_5PPh_2$), 4.84 (m, 2H, η^6-$C_6H_5PPh_2$), 6.02 (m, 1H, (η^6-C_6H_5)PPh$_2$). ^{31}P{^{1}H} (CD_2Cl_2, 162 MHz, 298 K): δ 50.2 (s, P$_{dppf}$), −8.1 (s, (η^6-C_6H_5)PPh$_2$). Selected ^{13}C{^{1}H} (CD_2Cl_2, 100 MHz, 298 K): δ 73.9 (m, C$_{dppf}$), 75.6 (m, C$_{dppf}$), 76.0 (m, C$_{dppf}$), 94.6 (dt, J_{CP} = 15.7 Hz, J_{CP} = 3.1 Hz, η^6-$C_6H_5PPh_2$), 97.1 (m, η^6-$C_6H_5PPh_2$), 96.3 (s, η^6-$C_6H_5PPh_2$), 109.7 (dt, J_{CP} = 27.4 Hz, J_{CP} = 2.1 Hz, η^6-$C_6H_5PPh_2$). Anal. Calcd (%) for $C_{84}H_{44}BF_{24}P_3FeRu\cdot CH_2Cl_2$ (1781.98): C 54.69, H 3.13; found: C 54.77, H 2.91.

[Ru(dppf)(PPh$_3$)(CO)$_2$H]BAr$^F_4$ (9). A solution of **8** (0.100 g, 0.057 mmol) in CH_2Cl_2 (10 mL) in an ampule fitted with a J. Young's PTFE valve was freeze−pump−thaw degassed three times, placed under 1 atm CO and heated at reflux for 15 h. After cooling, the solvent was removed, and the resulting orange solid washed with hexane (2 × 10 mL) to give **9** as a yellow solid, which was spectroscopically characterized (Yield: 0.058 g, 56%). Selected ^{1}H NMR (CD_2Cl_2, 400 MHz, 298 K): δ −8.56 (ddd, $^2J_{HP}$ = 62.2 Hz, $^2J_{HP}$ = 24.3 Hz, $^2J_{HP}$ = 19.3 Hz, 1H, RuH: ^{1}H{^{31}P} NMR spectrum recorded with ^{13}CO labeling: δ −8.56 (t, $^2J_{HC}$ = 5.6 Hz)), 4.25 (s, 2H, C_5H_4), 4.49 (s, 2H, C_5H_4), 4.52 (s, 2H, C_5H_4), 4.62 (m, 2H, C_5H_4). ^{31}P{^{1}H} (CD_2Cl_2, 162 MHz, 298 K): δ 36.8 (dd, $^2J_{PP}$ = 178 Hz, $^2J_{PP}$ = 13 Hz), 32.3 (dd, $^2J_{PP}$ = 178 Hz, $^2J_{PP}$ = 17 Hz), 20.4 (dd, $^2J_{PP}$ = 17 Hz, $^2J_{PP}$ = 13 Hz). Selected ^{13}C{^{1}H} (CD_2Cl_2, 100 MHz, 298 K): δ 200.2 (dt, $^2J_{CP}$ = 14.1 Hz, $^2J_{CP}$ = 11.1 Hz, CO). IR (CH_2Cl_2, cm^{-1}): 2001 (ν_{CO}). ESI-TOF MS: [M]$^+$ m/z = 975.0980 (theoretical 975.0958).

[Ru(PMe$_3$)$_5$H]BAr$_4^F$ (10). PMe$_3$ (0.077 mL, 0.75 mmol) was added by syringe to a THF (10 mL) solution of **8** (0.267 g, 0.15 mmol) in an ampule fitted with a J. Young's PTFE valve, and the reaction mixture heated at reflux for 3 h. After cooling, the solvent was removed, and the resulting pale yellow solid washed with benzene (2 × 10 mL) and recrystallized from THF/hexane to afford **10** as clear needle-like crystals (0.100 g, 50%). ^{1}H NMR (THF-d_8, 500 MHz, 298 K): δ −11.35 (dquin, $^2J_{HP}$ = 74.4 Hz, $^2J_{HP}$ = 25.3 Hz, 1H, RuH), 1.38 (d, 9H, $^2J_{HP}$ = 5.9 Hz, PMe$_3$), 1.54 (br s, 36H, PMe$_3$). ^{31}P{^{1}H} (THF-d_8, 201 MHz, 298 K): δ −23.2 (quint, $^2J_{PP}$ = 26 Hz), −9.9 (d, $^2J_{PP}$ = 26 Hz). Anal. Calcd (%) for $C_{47}H_{58}BF_{24}P_5Ru$ (1345.69): C 41.95, H 4.34; found: C 41.86, H 4.28.

X-ray Crystallography. Single crystals of compounds for **1a**−**d**, **2a**, **3a**, **5a**, **5b**, **8**, and **10** were analyzed at using Mo($K\alpha$) radiation. Data collection for **10** was also effected at 100 K on an Oxford Diffraction Gemini diffractometer, whereas all other data sets were collected at 150 K on a Nonius Kappa CCD machine. Details of the data collections, solutions, and refinements are given in Table 1. The structures were solved using SHELXS-97[16] and refined using full-matrix least-squares in SHELXL-97.[16]

Refinements were generally straightforward, and hydride ligands, where located, were refined at a distance of 1.6 Å from the central ruthenium atom. The following points merit noting. The structure of **1a** was seen to contain two benzene molecules in addition to 1 molecule of the ruthenium complex in the asymmetric unit, while in **1b**, two molecules of CH_2Cl_2 were in evidence in the motif. Optimal refinement was achieved after accounting for disorder of one chlorine in each solvent moiety. A solvent fragment of dichloromethane (75% occupancy) was found in **1c**. In **1d**, the asymmetric unit was found to contain

(16) Sheldrick, G. M. *Acta Crystallogr.* **1990**, *467*−*473*, A46. Sheldrick, G. M. *SHELXL-97, a computer program for crystal structure refinement*; University of Göttingen: Göttingen, Germany, 1997.

Table 1. Crystal Data for Complexes **1a**, **1b**, **1c**, **2a**, **3a**, **5a**, **5b**, **1d**, **8**, and **10**

	1a	**1b**	**1c**	**2a**	**3a**	**5a**
empirical formula	$C_{69}H_{60}ClOP_3Ru$	$C_{56}H_{48}Cl_5OP_3Ru$	$C_{46.75}H_{45.5}C_{12.5}OP_3Ru$	$C_{60.70}H_{53.40}Cl_{5.40}F_3O_4P_3RuS$	$C_{92.6}H_{62}BF_{24}O_2P_3Ru$	$C_{89.5}H_{61}BClF_{24}O_3P_3Ru$
formula weight	1134.60	1108.17	905.94	1321.30	1867.41	1880.62
crystal system	monoclinic	monoclinic	monoclinic	triclinic	monoclinic	monoclinic
space group	$P2_1/n$	$P2_1/a$	$P2_1/n$	$P\bar{1}$	$P2_1/a$	$P2_1/a$
a/Å	13.3340(1)	12.0690(1)	9.8590(1)	12.9730(1)	18.4540(2)	13.2770(1)
b/Å	30.1610(3)	36.7400(3)	26.7330(4)	14.8850(1)	20.4010(3)	40.2040(4)
c/Å	14.0980(2)	12.1330(1)	16.7610(3)	15.5800(2)	22.4910(3)	17.2050(2)
α/deg	90	90	90	86.635(1)	90	90
β/deg	96.471(1)	109.006(1)	103.583(1)	84.018(1)	94.387(1)	97.14
γ/deg	90	90	90	80.954(1)	90	90
U/Å^3	5633.62(11)	5086.66(7)	4293.98(11)	2952.21(5)	8442.60(19)	9112.55(16)
Z	4	4	4	2	4	4
D_c/g cm^{-3}	1.338	1.447	1.401	1.486	1.469	1.371
μ/mm^{-1}	0.455	0.705	0.667	0.683	0.345	0.349
F(000)	2352	2264	1862	1347	3774	3796
crystal size/mm	0.45 × 0.40 × 0.25	0.32 × 0.20 × 0.12	0.25 × 0.07 × 0.07	0.30 × 0.25 × 0.25	0.25 × 0.15 × 0.07	0.30 × 0.15 × 0.05
θ min., max for data collection	3.52, 30.07	3.55, 27.48	3.72, 27.49	3.55, 30.00	3.52, 25.03	3.52, 25.00
index ranges	$-18 \le h \le 18$; $-42 \le k \le 42$; $-19 \le l \le 19$	$-15 \le h \le 15$; $-47 \le k \le 47$; $-15 \le l \le 15$	$-12 \le h \le 12$; $-34 \le k \le 34$; $-21 \le l \le 21$	$-18 \le h \le 18$; $-20 \le k \le 20$; $-21 \le l \le 21$	$-21 \le h \le 21$; $-24 \le k \le 24$; $-26 \le l \le 26$	$-15 \le h \le 15$; $-47 \le k \le 47$; $-20 \le l \le 20$
reflections collected	70022	50533	67435	67721	119161	126839
independent reflections, R_{int}	16368, 0.1263	11498, 0.0656	9827, 0.0538	17100, 0.0424	14858, 0.1470	15997, 0.1394
reflections observed (> 2σ)	9135	9373	8020	14227	11104	10693
data completeness	0.990	0.986	0.996	0.995	0.997	0.996
absorption correction	multiscan	multiscan	multiscan	multiscan	multiscan	multiscan
max., min transmission	0.90, 0.78	0.94, 0.88	0.894, 0.829	0.900, 0.801	0.987, 0.559	0.973, 0.868
data/restraints/parameters	16368/4/682	11498/1/614	9827/1/501	17100/6/730	14858/131/1210	15997/199/1172
goodness-of-fit n F^2	1.004	1.018	1.099	1.028	1.034	1.110
final $R1$, $wR2$ [$I > 2\sigma(I)$]	0.0564, 0.1048	0.0432, 0.1038	0.0442, 0.1039	0.0433, 0.1108	0.0502, 0.1184	0.0963, 0.2347
final $R1$, $wR2$ (all data)	0.1363, 0.1295	0.0588, 0.1126	0.0605, 0.1109	0.0560, 0.1195	0.0761, 0.1382	0.1470, 0.2625
largest diff. peak, hole/e Å^{-3}	1.471, −0.540	1.624, −1.343	1.417, −0.474	0.684, −0.521	0.684, −0.521	0.854, −0.704

	5b	**1d**	**8**	**10**
empirical formula	$C_{86}H_{56}BF_{24}O_3P_3Ru$	$C_{64}H_{68}ClFeO_3P_3Ru$	$C_{84}H_{56}BF_{24}FeP_3Ru$	$C_{62.75}H_{80.50}B_{1.25}F_{30}OP_{6.25}Ru_{1.25}$
formula weight	1798.10	1170.46	1781.93	1754.18
crystal system	triclinic	triclinic	monoclinic	tetragonal
space group	$P\bar{1}$ (No. 2)	$P\bar{1}$ (No. 2)	$P2_1/c$	$P4_2/n$
a/Å	12.9450(3)	11.4620(1)	10.4940(1)	29.3244(2)
b/Å	15.8550(4)	15.0460(2)	39.4160(5)	29.3244(2)
c/Å	19.7860(5)	16.2070(2)	19.0500(2)	17.9383(2)
α/deg	101.010(2)	100.190(1)	90	90
β/deg	91.365(1)	93.125(1)	100.025(1)	90
γ/deg	90.110(1)	97.346(1)	90	90
U/Å^3	3984.97(17)	2719.82(5)	7759.37(15)	15425.5(2)
Z	2	2	4	8
D_c/g cm^{-3}	1.499	1.429	1.525	1.511
μ/mm^{-1}	0.363	0.729	0.547	0.491
F(000)	1812	1216	3584	7120
crystal size/mm	0.20 × 0.20 × 0.12	0.25 × 0.20 × 0.20	0.15 × 0.15 × 0.12	0.35 × 0.35 × 0.24
θ min., max for data collection	3.55, 27.47	3.51, 27.52	3.61, 27.53	2.75 to 27.48
index ranges	$-16 \le h \le 16$; $-18 \le k \le 19$; $-22 \le l \le 25$	$-14 \le h \le 14$; $-19 \le k \le 19$; $-20 \le l \le 21$	$-13 \le h \le 13$; $-51 \le k \le 51$; $-24 \le l \le 24$	$-38 \le h \le 38$; $-38 \le k \le 38$; $-23 \le l \le 23$
reflections collected	22391	55440	98604	253414
independent reflections, R_{int}	15058, 0.0389	12442, 0.0580	17766, 0.0633	17670, 0.0412
reflections observed (> 2σ)	11363	9843	12706	12713
data completeness	0.824	0.995	0.994	0.999
absorption correction	multiscan	multiscan	multiscan	multiscan
max., min transmission	0.927, 0.895	0.870, 0.821	0.901, 0.829	1.000 and 0.944
data/restraints/parameters	15058/151/1115	12442/1/662	17766/121/1099	17670/139/898
goodness-of-fit n F^2	1.047	1.053	1.027	1.094

three THF molecules in addition to one molecule of the complex. The structure of **2a** also fell prey to lattice solvent. Within the asymmetric unit, two full molecules of dichloromethane were in evidence, along with an additional region of electron density that was modeled as 0.7 of a CH_2Cl_2 molecule. The latter was split over two sites in a 50:20 ratio and, to assist convergence, C−Cl and Cl···Cl distances were restrained in the disordered region.

Compound **3a** proved challenging from a solid-state characterization perspective, the sample in this case, a thin plate,

Scheme 1

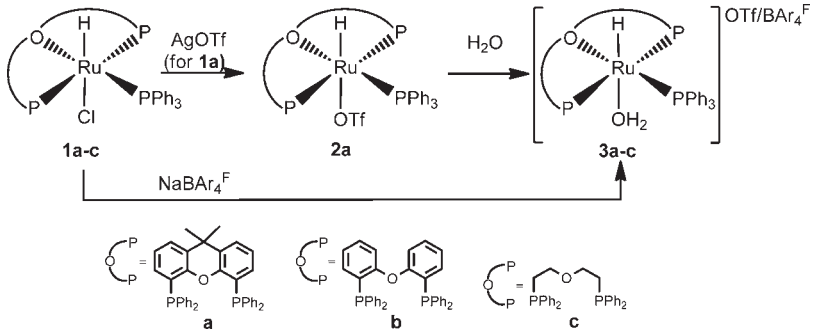

being of less than ideal quality. The asymmetric unit was seen to comprise one cation, one anion, and a hopeless region of disordered solvent. The hydrogen atoms in the ligated water were located with reasonably convincing credibility, and refined at 0.89 Å from O2, 1.6 Å from each other, and equidistant from Ru1. Disorder reigned in relation to the fluorines in the anion. In particular, the halogens in the CF_3 groups containing F10, F19, and F22 exhibited 65:35 disorder, while the fluorines in the group containing F16 were shown to have 50:50 disorder. C−F and F−F distances in disordered regions were refined subject to similarity restraints. Fractional fluorines with occupancy of less than 50% were treated isotropically. The solvent region in this structure is best described as "messy". Ultimately this region was modeled as partial carbon atoms (i.e., a fractional pentane of recrystallization) with the hydrogens not included in this region.

In **5a**, the asymmetric unit was seen to be constituted by one cation, one anion, and a solvent fragment that approximates to half of a molecule of dichloromethane. Disorder was prevalent in all three species. Specifically, the phenyl rings containing carbons 16−21 and 22−26 were disordered over 2 sites in a 1:1 ratio. These partial rings were treated as rigid hexagons in the refinement. Unsurprisingly, some of the CF_3 groups in the anion also exhibited disorder. Those fluorine atoms attached to C81 and C88 were found to be disordered in site-occupancy ratios of 55:45 and 50:50 respectively. C−F and F···F distances were restrained in these disordered functionalities during the final least-squares cycles. Partial atoms with occupancies of 50% or greater were refined anisotropically, subject to restraints. The solvent was diffuse, and difficulties in modeling same were overcome by employing the PLATON "SQUEEZE" function.[17] On this basis, half of a CH_2Cl_2 molecule has been included in the asymmetric unit for this structure.

The sample for **5b** crystallized as flat plates, and this is evidenced, in part, by the *R*(int) for the data which were truncated at a θ value of 25°. There was no solvent present in **8**, but the central ruthenium in the cation exhibited 75:25 disorder over two sites, both of which were treated anisotropically. A credible hydride position was evident in the difference Fourier electron density map, and this was refined, as described above, at 1.6 Å from the 75% occupancy metal, rather than split over 2 sites. Some of the fluorines in the anion also exhibited disorder. In particular, F1-3/F1A-3A, F7-9/F7A-9A, F10-12/F10A-12A, and F13-15/F13A-15A refined with disorder ratios of 65:35, 55:45, 65:35, and 80:20, respectively. C−F and F···F distances in disordered CF_3 groups were refined subject to distance similarity restraints.

The structure of **10** was somewhat tricky to finalize. An initial data collection revealed that the asymmetric unit contained one full cation, one full anion, one-quarter of an anion (with the central boron, B2, located on a special position bearing −4 symmetry), and one-quarter of a cation. The first three of these components refined easily, but the cation quarter represented a catastrophe in terms of modeling. The forced −4 symmetry position close to the ruthenium at the center of this moiety forced geometrical restraints which do not coincide with the point group symmetry of a full cation. Hence, disorder was rife, and could not be modeled sensibly. It became evident therefore, that to effect a good convergence, this region would need to be treated with the PLATON SQUEEZE function. However, before taking this pathway, an optimal quality data set is necessary, and hence, a second collection ensued. Refinement of the structure using these new data revealed a very disordered molecule of THF to also be present within the asymmetric unit. Rigorous attempts were made to model the two disordered regions, but to no avail. Lower symmetry space group possibilities plus twinning were also considered, but these alternatives caused convergence deterioration. Moreover, the electron density map region pertaining to the second cation could not be resolved any better, even at the very lowest of the symmetries interrogated. Thus, SQUEEZE was employed, and because of the data quality, there is good agreement between the calculated electron counts in the voids and the chemical model evident before using this algorithm. The unit cell contents presented herein take account of the "squeezed" solvent and cation quarter. Some disorder of the CF_3 groups was also modeled successfully in this structure. In particular, the fluorines attached to C39, C45, C54, and C55 were seen to be disordered in the following ratios, respectively: 75:25; 60:40; 65:35, and 55:45. C−F and F···F distances in disordered functionalities were refined subject to restraints and only partial fluorines with greater than 50% occupancy were refined anisotropically.

Crystallographic data for compounds **1a** (766186), **1b** (766187), **1c** (766188), **2a** (780097), **3a** (766189), **5a** (766190), **5b** (766191), **1d** (766192), **8** (766193), and **10** (766194) have been deposited with the Cambridge Crystallographic Data Center as supplementary publications. Copies of the data can be obtained free of charge on application to CCDC, 12 Union Road, Cambridge CB2 1EZ, U.K. [fax(+44) 1223 336033, e-mail: deposit@ccdc.cam.ac.uk].

Results and Discussion

Synthesis and Characterization of Ru(P−O−P)(PPh_3)HCl (1a−c). The chelating phosphine precursors Ru(P−O−P)(PPh_3)HCl (xantphos, **1a**; DPephos, **1b**; ($Ph_2PCH_2CH_2$)$_2$O, **1c**) were prepared by refluxing Ru(PPh_3)$_3$HCl with 1−3 equiv of the appropriate phosphine ligands in THF, and isolated as mildly air-sensitive orange solids in good to excellent yields (60−90%). The $^{31}P\{^1H\}$ NMR spectra of **1a** and **1c** displayed a triplet signal for the triphenylphosphine ligand at δ 75.2 and δ 71.0 respectively, along with a lower frequency doublet resonance at δ 46.7 (**1a**) and δ 42.3 (**1c**) arising from the coordinated

(17) Spek, A. L. A *Multipurpose Crystallographic Tool*; Utrecht University: Utrecht, The Netherlands, 2001.

P−O−P ligands. The splitting patterns and coupling constants ($^2J_{PP}$ ca. 33 Hz) are consistent with **1a**−**c** adopting *mer* P−O−P geometries as shown in Scheme 1. In the case of **1b**, the phosphorus resonances of the DPEphos ligand appeared as a broad singlet at room temperature, but resolved upon cooling to 230 K into an ABX spin system with a trans $^2J_{PP}$ coupling of 285 Hz. The non-equivalence of the two P-atoms within the chelate arises from a conformation of the complexed ligand in which the four P-phenyl groups adopt pseudo-axial and pseudo-equatorial positions. The ^{1}H NMR spectra of the three complexes all exhibited a single hydride resonance (**1a**: δ −16.22; **1b**: δ −16.34; **1c**: δ −17.54) with a doublet of triplets multiplicity. The magnitude of the J_{HP} couplings indicate a cis disposition of hydride with respect to both the chelating phosphines and the PPh_3 ligands.

The molecular structures of **1a**−**c** were determined by X-ray crystallography and are displayed in Figure 1, with pertinent bond lengths and angles listed in Table 2. In all of the structures, the chelating phosphines are coordinated through all three POP atoms in a *mer*-configuration with trans P−Ru−P angles between 156 and 158°. Coordination of the oxygen atom is presumably desirable in allowing the complexes to achieve 18-electron counts. It is notable that in **1a** and **1b** there is substantial evidence for intramolecular π stacking involving one phenyl ring from the chelating phosphine and another from the triphenylphosphine ligand. In particular, the shortest distances between the mean planes of the rings based on C29 and C41 in **1a** and C25 and C37 in **1b** are 3.28 and 3.24 Å, respectively. The Ru−$P_{chelate}$ distances (2.29−2.34 Å) are considerably longer than the Ru−PPh_3 distances (all ca. 2.22 Å), while the Ru−O distances lie within the range 2.25−2.28 Å.

Chloride Abstraction from 1a−c. Treatment of dichloromethane solutions of **1a**−**c** with 1.1 equiv of $NaBAr_4^F$ (BAr_4^F = B(3,5-$C_6H_3(CF_3)_2)_4$) resulted in abstraction of the chloride ligands and the appearance of hydride signals for the products **3a**−**c** at lower frequencies (δ −19.67, δ −18.67, and δ −21.05) than found in the neutral starting materials. This is consistent with **3a**−**c** having hydride ligands either trans to a vacant coordination site (i.e., as in the 16e species [Ru(P−O−P)(PPh_3)H]$^+$) or trans to a weakly bound solvent molecule (i.e., as the 18e species [Ru(P−O−P)(PPh_3)(solvent)H]$^+$).[18] Although an X-ray structure of a crystal of **3a** isolated (serendipitously!) from a reaction of **1a** with $NaBAr_4^F$ revealed a loosely bound water molecule (Ru−OH_2 = 2.32(5) Å)[19] in the sixth coordination site on the metal (Figure 3), we sought conclusive evidence for solvent coordination in the bulk material in solution.

(18) (a) Esteruelas, M. A.; Werner, H. *J. Organomet. Chem.* **1986**, *303*, 221–231. (b) Salem, H.; Shimon, L. J. W.; Diskin-Posner, Y.; Leitus, G.; Ben-David, Y.; Milstein, D. *Organometallics* **2009**, *28*, 4791–4806.

(19) For comparisons, see for example: (a) Boniface, S. M.; Clark, G. R.; Collins, T. J.; Roper, W. R. *J. Organomet. Chem.* **1981**, *206*, 109–117. (b) Harding, P. A.; Robinson, S. D.; Henrick, K. *J. Chem. Soc., Dalton Trans.* **1988**, 415–420. (c) Goicoechea, J. M.; Mahon, M. F.; Whittlesey, M. K.; Kumar, P. G. A.; Pregosin, P. S. *Dalton Trans.* **2005**, 588–597. (d) Zhang, J.; Gandelman, M.; Shimon, L. J. W.; Milstein, D. *Dalton Trans.* **2007**, 107–113. (e) Szymczak, N. K.; Braden, D. A.; Crossland, J. L.; Turov, Y.; Zakharov, L. N.; Tyler, D. R. *Inorg. Chem.* **2009**, *48*, 2976–2984.

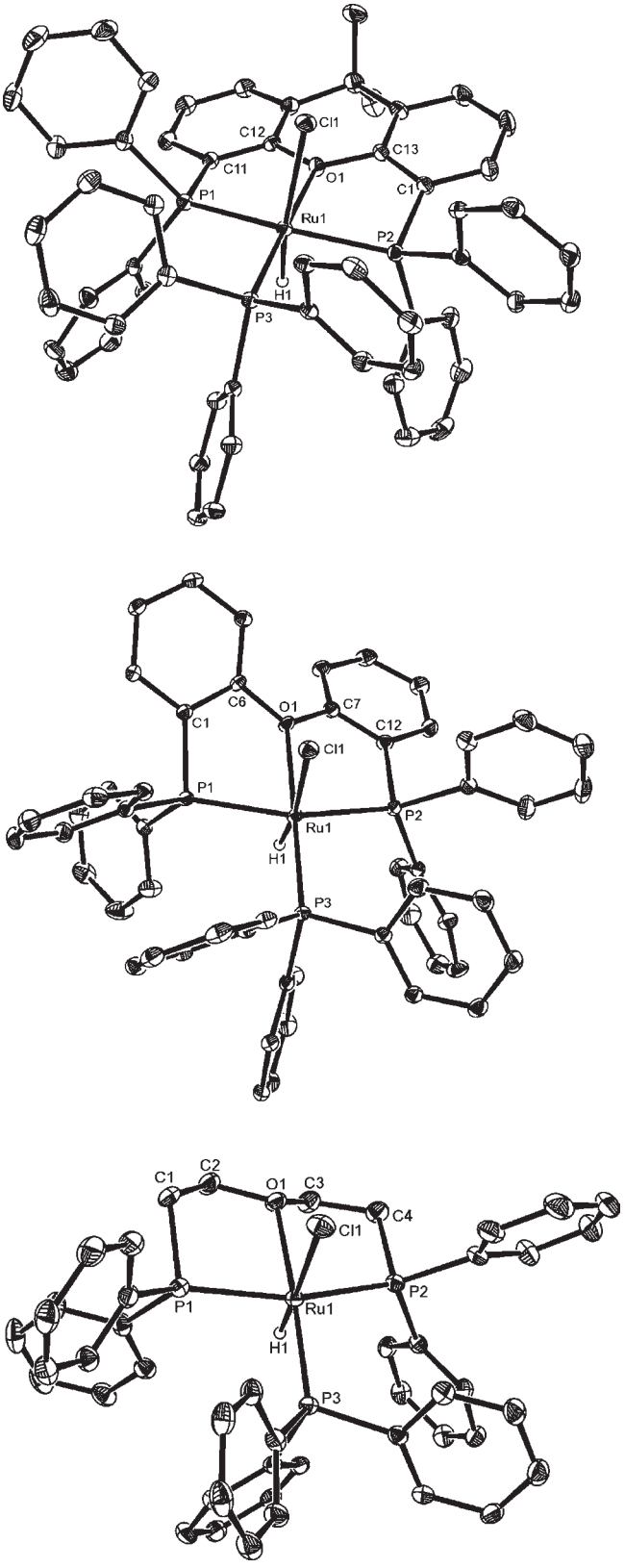

Figure 1. Molecular structures of Ru(xantphos)(PPh_3)HCl (**1a**), Ru(DPEphos)(PPh_3)HCl (**1b**), and Ru(($Ph_2PCH_2CH_2)_2O$)(PPh_3)HCl (**1c**). Thermal ellipsoids are shown at 30% level. Solvent moieties and all hydrogen atoms, except Ru−H, are omitted for clarity.

A series of NMR experiments proved beyond doubt that **3a**−**c** are the aqua complexes [Ru(P−O−P)(PPh_3)(H_2O)H]$^+$. Thus, a proton NMR spectrum of **3a** recorded

Table 2. Selected Bond Lengths (Å) and Angles (deg) for Ru(xantphos)-(PPh_3)HCl (**1a**), Ru(DPEphos)(PPh_3)HCl (**1b**), and Ru(($Ph_2PCH_2CH_2)_2O$)-(PPh_3)HCl (**1c**)

	1a	1b	1c
Ru(1)−P(1)	2.3037(8)	2.3319(7)	2.3085(9)
Ru(1)−P(2)	2.3060(8)	2.2918(7)	2.3364(8)
Ru(1)−P(3)	2.2277(8)	2.2271(7)	2.2292(8)
Ru(1)−O(1)	2.2509(19)	2.2480(17)	2.278(2)
Ru(1)−Cl(1)	2.5200(8)	2.5120(7)	2.5192(9)
P(1)−Ru(1)−P(2)	156.39(3)	156.52(3)	158.31(3)
P(1)−Ru(1)−P(3)	98.66(3)	101.76(2)	98.91(3)
P(2)−Ru(1)−P(3)	100.18(3)	98.52(3)	99.48(3)
O(1)−Ru(1)−P(3)	176.46(6)	177.05(6)	171.08(6)
Cl(1)−Ru(1)−P(3)	100.16(3)	96.82(2)	101.63(3)

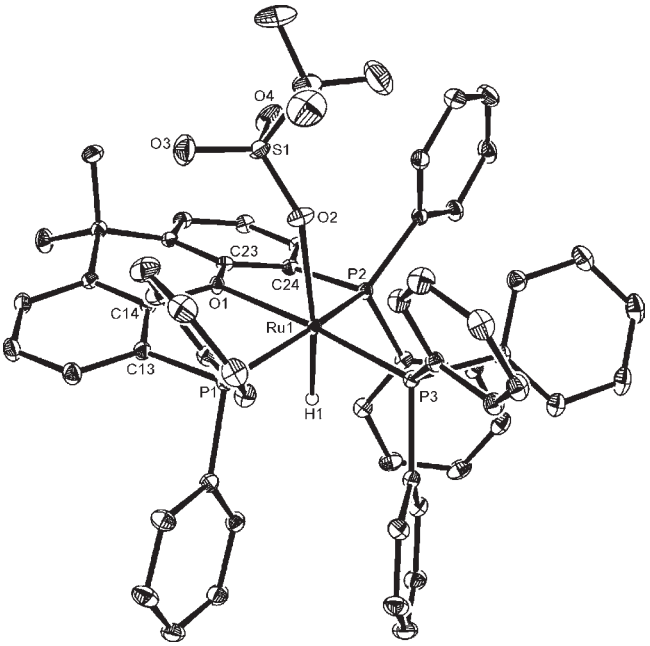

Figure 2. Molecular structure of Ru(xantphos)(PPh_3)H(OTf) (**2a**). Thermal ellipsoids are shown at 30% level. All hydrogen atoms, except Ru−H, are omitted for clarity. Selected bond lengths (Å) and angles (deg): Ru(1)−P(1) 2.3062(6), Ru(1)−P(2) 2.3118(5), Ru(1)−P(3) 2.2424(6), Ru(1)−O(1) 2.2563(15), Ru(1)−O(2) 2.3139(17), P(1)−Ru(1)−P(2) 156.72(2), P(1)−Ru(1)−P(3) 96.72(2), P(2)−Ru(1)−P(3) 98.92(2), O(1)−Ru(1)−P(3) 175.34(4), O(1)−Ru(1)−O(2) 81.50(6).

immediately after reaction of **1a** with $NaBAr_4^F$ in degassed, but undried, dichloromethane showed a single Ru−H resonance with the same chemical shift value (δ −19.67) reported above, although the signal was broad and devoid of any resolvable couplings to phosphorus, suggestive of exchange.[20] Moreover, when 2 equiv of water were added to a CD_2Cl_2 solution of the triflate complex Ru(xantphos)(PPh_3)H(OTf) (**2a**, Figure 2), the initial Ru−H signal of **2a** at δ −22.27[21] shifted to higher frequency (δ −21.81) and broadened. With a total of 10 equiv of water present, the hydride resonance appeared at even higher frequency, δ −19.98. As expected, a more coordinating solvent such as acetonitrile was also able to displace the triflate ligand from **2a** to give [Ru(xantphos)(PPh_3)-(MeCN)H]OTf (**4a**). Thus, addition of MeCN (5 equiv) to

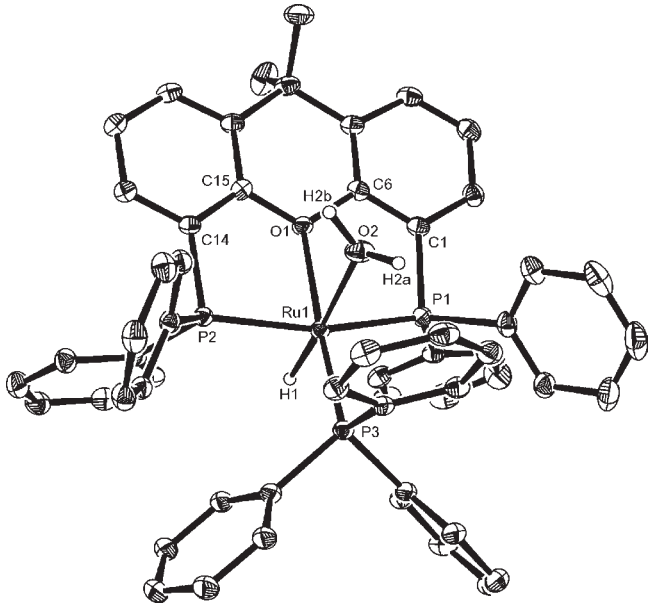

Figure 3. Structure of the cation in [Ru(xantphos)(PPh_3)(H_2O)H]-BAr_4^F (**3a**). Thermal ellipsoids are shown at 30% level. All hydrogen atoms, except Ru−H and Ru−OH_2, are omitted for clarity. Selected bond lengths (Å) and angles (deg): Ru(1)−P(1) 2.306(13), Ru(1)−P(2) 2.298(13), Ru(1)−P(3) 2.228(13), Ru(1)−O(1) 2.25(3), Ru(1)−O(2) 2.32(4), P(1)−Ru(1)−P(2) 160.1(5), P(1)−Ru(1)−P(3) 99.4(5), P(2)−Ru(1)−P(3) 99.5(5), O(1)−Ru(1)−P(3) 173.1(10).

2a in CD_2Cl_2 produced a new hydride signal at even higher frequency, δ −13.42, assigned to **4a**; a comparable chemical shift (δ −13.39) was observed when 5 equiv of MeCN were added to a sample of **1a**/ $NaBAr_4^F$. More definitive evidence for acetonitrile coordination came from the observed proton singlet at δ 1.36, together with carbon resonances at δ 2.9 and 121.8, and finally, a band corresponding to ν_{CN} at 2241 cm^{-1} in the IR spectrum.

Reaction of 3a−c with O_2. Exposure of CH_2Cl_2 solutions of **3a−c** to air at room temperature led to the rapid (and irreversible) formation of the cationic dioxygen hydride complexes [Ru(P−O−P)(PPh_3)(η^2-O_2)H]BAr_4^F (**5a−c**), which were isolated and structurally characterized in the cases of xantphos (**5a**) and DPEphos (**5b**). Yellow solutions of complex **5c** rapidly reveal a green tint suggesting oxidation to Ru(III). Similar green solutions were also observed with the xantphos and DPEphos derivatives if they were formed by reaction with O_2 rather than air.

The ^{1}H NMR spectra of **5a−c** all display hydride signals at a relatively high frequency between δ −1.5 and δ −3 as a doublet of triplets with $^2J_{HP}$ values in the range 26−32 Hz, consistent with structures shown in Scheme 2 in which O_2 is coordinated trans to hydride. All three chemical shifts are intermediate between the value of δ −5.8 for [Ru(^{i}Pr$_2$PCH$_2$CH$_2$P^{i}Pr$_2$)$_2$(η^2-O_2)H]$^+$ and the positive value of δ 4.8 reported recently for the N-heterocyclic carbene species [Ru(I^{i}Pr$_2$Me$_2$)$_4$(η^2-O_2)H]$^+$ (I^{i}Pr$_2$Me$_2$ = 1,3-diisopropyl-4,5-dimethylimidazol-2-ylidene).[22−24] In the ^{31}P{^{1}H} NMR spectra, the coordination of oxygen leads to similar chemical shifts for both the chelating

(20) We were unable to identify resonances arising from the coordinated water ligand.

(21) Upon warming to 315 K, we observed sharpening of the resonance to the expected doublet of triplets multiplicity.

(22) Jiménez-Tenorio, M.; Puerta, M. C.; Valerga, P. *J. Am. Chem. Soc.* **1993**, *115*, 9794–9795.

(23) Jiménez-Tenorio, M.; Puerta, M. C.; Valerga, P. *Inorg. Chem.* **1994**, *33*, 3515–3520.

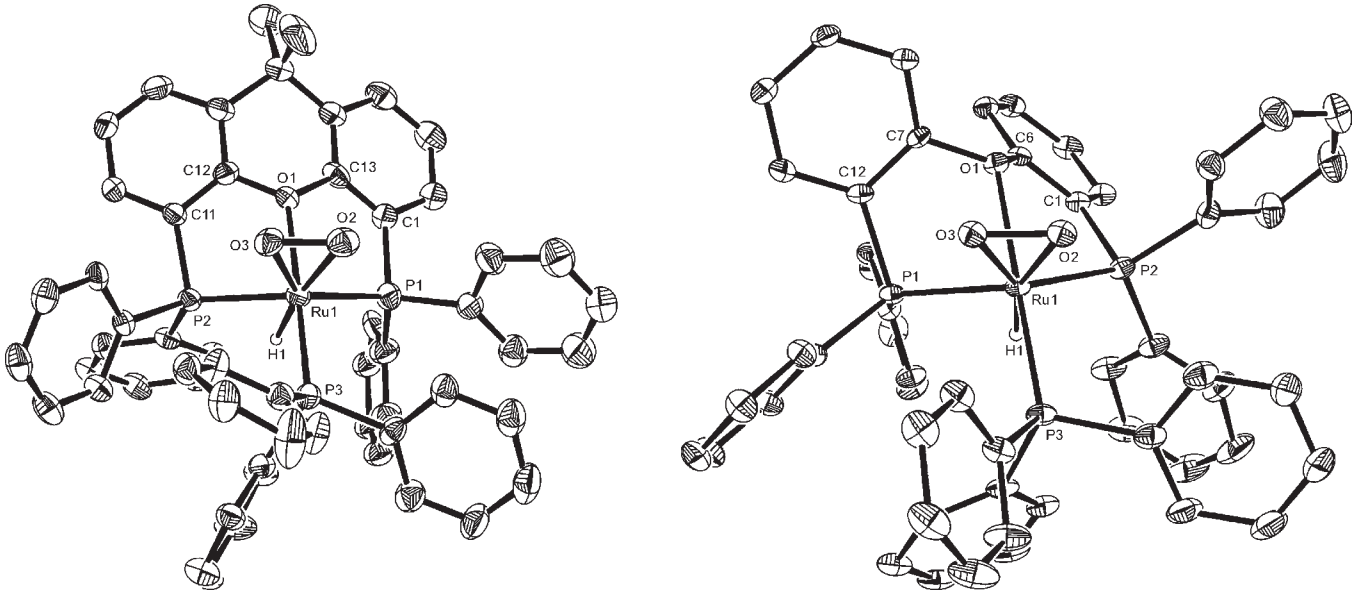

Figure 4. Molecular structures of the cations in $[Ru(xantphos)(PPh_3)(\eta^2\text{-}O_2)H]BAr_4^F$ (**5a**) and $[Ru(DPEphos)(PPh_3)(\eta^2\text{-}O_2)H]BAr_4^F$ (**5b**). Thermal ellipsoids are shown 30% level. All hydrogen atoms, except Ru−H, are omitted for clarity. Selected bond lengths (Å) and angles (deg) for **5a**: Ru(1)−P(1) 2.339(2), Ru(1)−P(2) 2.3493(19), Ru(1)−P(3) 2.2883(19), O(2)−O(3) 1.453(7), Ru(1)−O(1) 2.257(4), Ru(1)−O(2) 2.006(5), Ru(1)−O(3) 2.026(5), P(1)−Ru(1)−P(2) 125.58(7), P(1)−Ru(1)−P(3) 102.49(7), P(2)−Ru(1)−P(3) 101.78(7), O(1)−Ru(1)−P(3) 176.79(13). For **5b**: Ru(1)−P(1) 2.3477(13), Ru(1)−P(2) 2.3294(13), Ru(1)−P(3) 2.2867(13), O(2)−O(3) 1.436(5), Ru(1)−O(1) 2.298(3), Ru(1)−O(2) 2.024(3), Ru(1)−O(3) 2.005(3), P(1)−Ru(1)−P(2) 119.48(4), P(1)−Ru(1)−P(3) 103.89(5), P(2)−Ru(1)−P(3) 102.20(5), O(1)−Ru(1)−P(3) 179.32(9).

Scheme 2

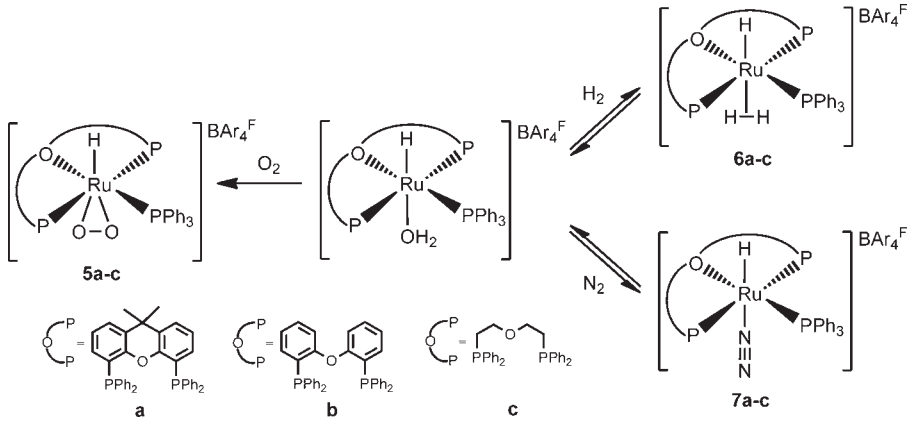

ligands and the PPh_3 groups (**5a**: δ 48.2, 44.4; **5b**: δ 41.4, 36.2; **5c** δ 48.2, 45.8). IR spectroscopy was uninformative as the $\nu_{(O-O)}$ stretches for both the $^{16}O_2$ and $^{18}O_2$ isotopomers of **5a** and **5b** were obscured by other absorption bands.

The molecular structures of **5a**−**b** are shown in Figure 4. The O−O distances of 1.453(7) (**5a**) and 1.436(5) Å (**5b**) are significantly longer than those reported in either $[Ru(dippe)_2(\eta^2\text{-}O_2)H]^+$ (1.360(10) Å; dippe = $^iPr_2PCH_2CH_2P^iPr_2$)[22,23] or $[Ru(I^iPr_2Me_2)_4(\eta^2\text{-}O_2)H]^+$ (1.354(5) Å),[24] but in the range for coordinated peroxide.[25] There are significant distortions to the xantphos and DPEphos ligands in **5a**−**b** compared with **1a**−**b**. Specifically, the P−Ru−P angle narrows dramatically from about 156° in the latter structures, to 125.58(7)° in **5a** and 119.48(4)° in **5b**. This change is concomitant with increased "hinging" of the xanthene about the O1−C6 axis in **5a** (angle between the aromatic ring mean planes is 149.3°) and in **5b** by the reduction in the P−O−P angle to 89.1° compared to 101.7° in **1b**.

Reaction of 3a−c with H_2 and D_2. Treatment of **1a**−**c** with $NaBAr_4^F$ in dichloromethane followed by addition of 1 atm H_2 afforded the thermally unstable dihydrogen hydride complexes $[Ru(P-O-P)(PPh_3)(\eta^2\text{-}H_2)H]BAr_4^F$ (**6a**−**c**), which were characterized by comparison of the Ru−H and Ru(η^2-H_2) chemical shifts to analogous ruthenium complexes in the literature.[26] The low frequency region of the ^1H NMR spectrum of $[Ru(xantphos)(PPh_3)(\eta^2\text{-}H_2)H]BAr_4^F$ (**6a**) recorded in CD_2Cl_2 at 180 K displayed a broad singlet at δ −0.95 arising from the η^2-H_2 ligand

(24) Häller, L. J. L.; Mas-Marzá, E.; Moreno, A.; Lowe, J. P.; Macgregor, S. A.; Mahon, M. F.; Pregosin, P. S.; Whittlesey, M. K. *J. Am. Chem. Soc.* **2009**, *131*, 9618–9619.

(25) (a) Vaska, L. *Acc. Chem. Res.* **1976**, *9*, 175–183. (b) Mezzetti, A.; Zangrando, E.; Del Zotto, A.; Rigo, P. *J. Chem. Soc., Chem. Commun.* **1994**, 1597–1598. (c) Yu, X.-Y.; Patrick, B. O.; James, B. R. *Organometallics* **2006**, *25*, 4870–4877; For a critical analysis of M-O_2 bonding, see: . Cramer, C. J.; Tolman, W. B.; Theopold, K. H.; Rheingold, A. L. *Proc. Natl. Acad. Sci. U.S.A.* **2003**, *100*, 3635–3640.

Table 3. NMR Data for [Ru(P−O−P)(PPh$_3$)(η^2-H$_2$)H]BAr$_4^F$ (**6a**−**c**)

compound	δ Ru(η^2-H$_2$)	δ/J_{HP} Ru−H	δ ^{31}P	T_1[c]
6a[a]	−0.95	−8.79 (22.4, 19.1 Hz)	67.6, 51.9	η^2-H$_2$: 9.0 ms (240 K)[d] H: 381 ms (239 K)[e]
6b[b]	−0.25	−7.95 (22.8, 19.4 Hz)	69.2, 47.1, 46.2	η^2-H$_2$: 9.6 ms (236 K)[d] H: 324 ms (239 K)[e]
6c[b]	−1.91	−9.16 (23.6, 16.2 Hz)	66.9, 56.2	η^2-H$_2$: 7.7 ms (224 K)[d] H: 273 ms (228 K)[e]

[a] Recorded at 180 K. [b] Recorded at 195 K. [c] Measured at 400 MHz. [d] $T_{1min\ values}$. [e] $T_{1(obs)}$ values at the closest recorded temperatures to the T_{1min} values of the dihydrogen ligands.

and a doublet of triplets at δ −8.79 ($^2J_{HP}$ = 22 and 19 Hz) for the terminal Ru−H. The similarity of J_{HP} to the values determined for **5a**−**c** suggests that the H$_2$ ligand lies trans to the hydride (Scheme 2). All three H−Ru(η^2-H$_2$) complexes were only stable under an atmosphere of hydrogen, and moreover, were present in equilibrium with the aqua precursors **3a**−**c**.[27] In the case of the xantphos species, the ratio of **6a**/**3a** was 3.8:1 at 180 K and 2.1:1 at 239 K.

Further evidence for assignment of **6a**−**c** as dihydrogen hydride complexes was provided by measurement of their spin−lattice relaxation times. A $T_{1\ min}$ value of 9 ms was determined for the η^2-H$_2$ ligand in the case of **6a** (240 K, 400 MHz), corresponding to an H−H separation of 0.98 or 0.78 Å for either a slow or a fast-spinning dihydrogen ligand.[28] As expected, the T_1 value for the terminal Ru−H was much longer. Table 3 summarizes the pertinent NMR data for the three dihydrogen hydride complexes.

Exposure of **3a**−**c** to 1 atm D$_2$ produced relatively complicated low temperature ^{1}H NMR spectra, with isotopic scrambling leading to the formation of a mixture of isotopomers. As shown in Figure 5 for the DPEphos complex **3b**, four resonances were seen in the hydride region of the ^{1}H{^{31}P} spectrum recorded at 180 K immediately after addition of D$_2$. After one day, the relative intensities of the four peaks had changed, with that at highest frequency decreasing and that at lowest frequency increasing. After degassing and addition of a fresh atmosphere of D$_2$, the intensities of the three lowest frequency signals all reduced, only to increase after a further 24 h. This variation of peak intensity as a function of time leads us to assign the highest frequency peak to [Ru(DPEphos)(PPh$_3$)(η^2-D$_2$)H]BAr$_4^F$, while that at the lowest frequency is assigned to the *dihydrogen* hydride species **6b**.[29,30] The formation of **6b** implies some form of H-D exchange process, most likely involving ortho-metalation

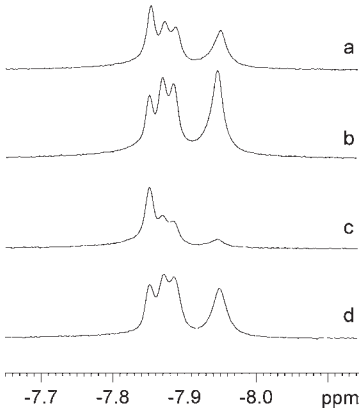

Figure 5. Hydride region of the ^{1}H {^{31}P} NMR spectrum (CD_2Cl_2, 400 MHz, 180 K) (a) immediately after addition of 1 atm D$_2$ to [Ru(DPEphos)(PPh$_3$)(H$_2$O)H]BAr$_4^F$ (**3b**), (b) after a further 24 h at room temperature, (c) after then being freeze−pump−thaw degassed and 1 atm D$_2$ reintroduced, and (d) a further 24 h later.

Scheme 3

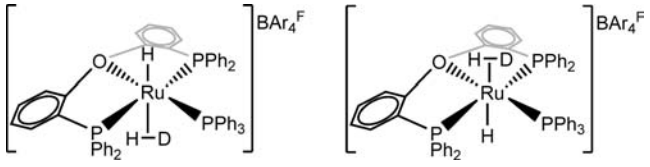

of the aryl group(s) on the phosphine ligand(s).[31] In support of this, deuterium incorporation into the aromatic region was apparent from the ^{2}H NMR spectrum. We propose that the two remaining signals arise from two isomers of [Ru(DPEphos)(PPh$_3$)(η^2-HD)H]BAr$_4^F$ in which the η^2-HD ligand sits on either side of the nonplanar DPEphos ligand, as shown in Scheme 3.[32]

The presence of the different HD isotopomers makes the dihydrogen region around δ −0.25 broad and unresolved, even with ^{31}P-decoupling. The experimental spectrum could be fitted with a simulation involving four η^2-HD isotopomers (arising as above from the η^2-HD ligand being either side of the DPEphos ligand and trans to either Ru−H or Ru−D) in which the 1:1:1 triplets partially overlap.[33] The simulated J_{HD} values range from 29.7 to 31.7 Hz, corresponding to an H−H separation of 0.89−0.92 Å. This is relatively close to the value for a slow-spinning dihydrogen ligand calculated on the basis of the $T_{1\ min}$ determination, although it is worth noting that in a recent summary of group 8 dihydrogen complexes,

(26) (a) Bautista, M. T.; Cappellani, E. P.; Drouin, S. D.; Morris, R. H.; Schweitzer, C. T.; Sella, A.; Zubkowski, J. *J. Am. Chem. Soc.* **1991**, *113*, 4876–4887. (b) Jia, G.; Drouin, S. D.; Jessop, P. G.; Lough, A. J.; Morris, R. H. *Organometallics* **1993**, *12*, 906–916. (c) Field, L. D.; Hambley, T. W.; Yau, B. C. K. *Inorg. Chem.* **1994**, *33*, 2009–2017. (d) Ogasawara, M.; Saburi, M. *J. Organomet. Chem.* **1994**, *482*, 7–14. (e) Schlaf, M.; Lough, A. J.; Morris, R. H. *Organometallics* **1997**, *16*, 1253–1259.

(27) For a discussion on the coordination of H$_2$O versus H$_2$, see: Kubas, G. J.; Burns, C. J.; Khalsa, G. R. K.; Van Der Sluys, L. S.; Kiss, G.; Hoff, C. D. *Organometallics* **1992**, *11*, 3390–3404.

(28) (a) Morris, R. H. *Coord. Chem. Rev.* **2008**, *252*, 2381–2394. (b) Morris, R. H. *Coord. Chem. Rev.* **2009**, *253*, 1219–1219.

(29) This resonance overlays perfectly that of **6b**.

(30) For a discussion of chemical shifts in partially deuterated hydride species, see: Oldham, W. J., Jr.; Hinkle, A. S.; Heinekey, D. M. *J. Am. Chem. Soc.* **1997**, *119*, 11028–11036.

(31) We assume that this involves metalation at the PPh$_3$ groups rather than the P−O−P ligands, but have not established this conclusively.

(32) Alternatively, there may be specific orientations of the η^2-HD ligand that cannot be interconverted. For example, the η^2-HD ligand could lie along the O−Ru−P vector with either the H or D over the Ru−O bond.

(33) See Supporting Information.

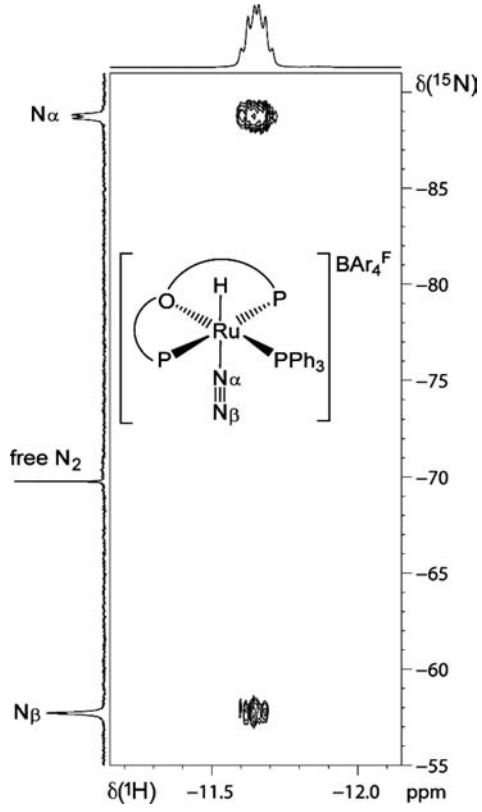

Figure 6. $^{1}H-^{15}N$ HMQC spectrum (700 MHz, CD_2Cl_2, 193 K) of $[Ru(xantphos)(PPh_3)(N_2)H]BAr_4^F$ (**7a**). Shown are the cross-peaks arising from the 2- and 3-bond correlations of the hydride ligand to N_α and N_β, respectively.

Morris reported that most of the trans $H-Ru(\eta^2-H_2)$ complexes in the literature contain an η^2-H_2 ligand in the fast-spinning regime.[28]

Reaction of 3a−c with N_2. Treatment of **1a−c** with $NaBAr_4^F$ followed by addition of 1 atm N_2 generated the trans-dinitrogen hydride complexes $[Ru(P-O-P)(PPh_3)(N_2)H]BAr_4^F$ (**7a−c**). As in the cases of **6a−c** discussed above, these species were only stable at low temperature under 1 atm N_2, and could therefore only be characterized spectroscopically by a combination of 1- and 2-D ^1H and ^{15}N NMR methods. The xantphos derivative **7a** is used to illustrate representative NMR data. It shows a hydride signal at δ −11.72 (180 K) that exhibits a relatively large trans J_{HN} doublet splitting of 18 Hz in the $^1H\{^{31}P\}$ NMR spectrum of a ^{15}N labeled sample. The 193 K $^{15}N\{^1H\}$ NMR spectrum of **7a** displayed two resonances at δ −88.7 and δ −57.6 which were assigned to the α- and β-N atoms, respectively, by comparison to the literature. Moreover, these chemical shifts point to **7a−c** being clear cases of mononuclear ruthenium complexes with end-on bound N_2 ligands.[34] Both signals displayed cross-peaks to the hydride resonance at δ −11.72 in the corresponding $^1H-^{15}N$ HMQC spectrum (Figure 6). A ^{15}N NMR saturation transfer experiment performed at 193 K on **7a** and **7b** revealed exchange between the complexed N_2 and free dinitrogen in solution. NMR data for the three dinitrogen hydride complexes **7a−c** are summarized in Table 4.

Table 4. NMR Data for $[Ru(P-O-P)(PPh_3)(N_2)H]BAr_4^F$ (**7a−c**)

compound	δ/J_{HP} Ru−H[a]	δ ^{31}P[a]	δ ^{15}N
7a	−11.72 (26.0, 16.5 Hz)	68.2, 47.8	−88.7, −57.6[b]
7b	−11.04 (26.7, 20.0 Hz)	65.4, 43.1, 41.7	−82.6, −51.8[b]
7c	−12.06 (25.3, 16.6 Hz)[c]	−67.2, 51.1[c]	−86.2, −59.1[c]

[a] Recorded at 180 K. [b] Recorded at 193 K. [c] Recorded at 195 K.

All three dinitrogen complexes were present in equilibrium with their aqua precursors. In the case of the xantphos derivative, for example, the ratio of **7a**/**3a** at 190 K was 6.7:1, but only 1.2:1 at 210 K. In the proton NMR spectrum at 266 K, only a very broad signal in the baseline corresponding to the hydride signal of **3a** was present.

In the reaction of **3a** with air to give **5a**, there was no trace of the dinitrogen complex **7a** found by NMR at low temperature indicating preferential binding of O_2 over N_2. Such a finding is consistent with previous experimental observations,[35] and also more recent computational studies on the coordination of the two molecules to $[Ru(NHC)_4H]^+$ and $[Ru(dippe)_2H]^+$.[36]

η^6-PPh_3 Coordination Upon Halide Abstraction from Ru(dppf)(PPh_3)HCl. In an attempt to establish the importance of the tridentate P−O−P coordination mode in allowing $[Ru(P-O-P)(PPh_3)(H_2O)H]^+$ to coordinate small molecules, we turned to the rigidly bidentate phosphine ligand dppf. The ruthenium complex Ru(dppf)-(PPh_3)HCl (**1d**) was formed as an orange, moderately air-stable solid in 48% yield by simply refluxing $Ru(PPh_3)_3$-HCl in the presence of 1 equiv of the ligand (Scheme 4).[37] As reported for the corresponding tricyclohexylphosphine analogue, Ru(dppf)(PCy_3)HCl,[38] **1d** is fluxional in solution. The ambient temperature $^{31}P\{^1H\}$ NMR spectrum displayed a broad singlet at δ 65 and a triplet at δ 41 assigned to the dppf and PPh_3 ligands, respectively. At 195 K, an ABX spin system was observed, with a large trans-J_{PP} coupling of 294 Hz associated with the PPh_3 and one of the dppf phosphorus signals. The data are consistent with a distorted trigonal bipyramidal arrangement found in Ru(dppf)(PCy_3)HCl. This was proven by an X-ray crystal structure determination, which is illustrated in Figure 7. The PPh_3 ligand and one arm of the dppf are indeed trans, occupying the apical positions of the tbp structure (P(1)−Ru−P(3), 159.45(3)°).[39] These apical Ru−P distances (Ru−P(1) 2.3587(7), Ru−P(3) 2.3086(7) Å) are significantly longer than the equatorial Ru−P bond length (Ru−P(2) 2.1850(7) Å).

Treatment of **1d** with $NaBAr_4^F$ failed to give an analogue of **3a−c**, but instead afforded $[Ru(dppf)\{(\eta^6-C_6H_5)-PPh_2\}H]BAr_4^F$ (**8**), in which the PPh_3 ligand is now coordinated through one of the aryl rings instead of the

(34) Donovan-Mtunzi, S.; Richards, R. L.; Mason, J. *J. Chem. Soc., Dalton Trans.* **1984**, 469–474.

(35) Jia, G.; Ng, W. S.; Chu, H. S.; Wong, W.-T.; Yu, N.-T.; Williams, I. D. *Organometallics* **1999**, *18*, 3597–3602.

(36) Burling, S.; Häller, L. J. L.; Mas-Marzá, E.; Moreno, A.; Macgregor, S. A.; Mahon, M. F.; Pregosin, P. S.; Whittlesey, M. K. *Chem.—Eur. J.* **2009**, *15*, 10912–10923.

(37) An alternative route to this material has been described in a patent. Rautenstrauch, V.; Challand, R.; Churlaud, R.; Morris, R. H.; Abdur-Rashid, K.; Brazi, E.; Mimoun, H. World Patent WO 2002022526 A2 20020321, 2002.

(38) Jung, S.; Brandt, C. D.; Werner, H. *Dalton Trans.* **2004**, 375–383.

(39) In $[Ru(dppf)(PPh_3)(CO)Cl]BF_4$, the bite angle of the dppf ligand expands to adopt a trans-spanning geometry. Kawano, H.; Nishimura, Y.; Onishi, M. *Dalton Trans.* **2003**, 1808–1812.

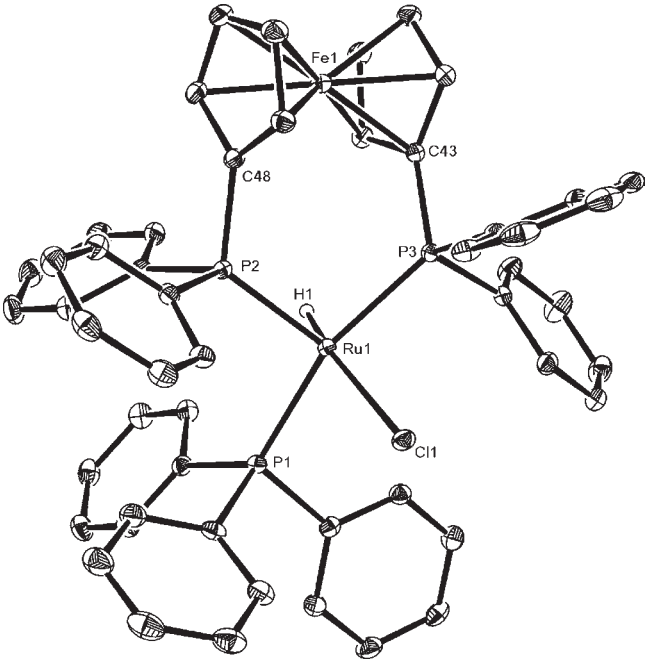

Figure 7. Molecular structure of Ru(dppf)(PPh_3)HCl (**1d**). Thermal ellipsoids are shown at 30% level. Solvent and all hydrogen atoms, except Ru−H, are omitted for clarity. Selected bond lengths (Å) and angles (deg): Ru(1)−P(1) 2.3587(7), Ru(1)−P(2) 2.1850(7), Ru(1)−P(3) 2.3086(7), Ru(1)−Cl(1) 2.4400(7), P(1)−Ru(1)−P(2) 98.84(3), P(1)−Ru(1)−P(3) 159.45(3), P(2)−Ru(1)−P(3) 99.96(3), Cl(1)−Ru(1)−P(2) 126.18(3).

Scheme 4

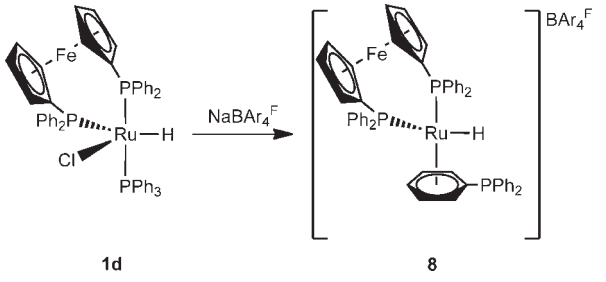

phosphorus atom (Scheme 4).[40−42] The X-ray crystal structure of **8** (Figure 8) reveals a distorted piano-stool arrangement of the η^6-arene, dppf, and hydride ligands around the ruthenium center. The coordinated arene is asymmetrically bound to the ruthenium, as evidenced by the longer (2.392(3) Å) Ru−C distance for the phosphorus bound carbon atom, compared with the average of the remaining Ru−C distances (2.23 Å).

Multinuclear NMR spectroscopy indicated that the structure of **8** was retained in solution. Two singlet resonances

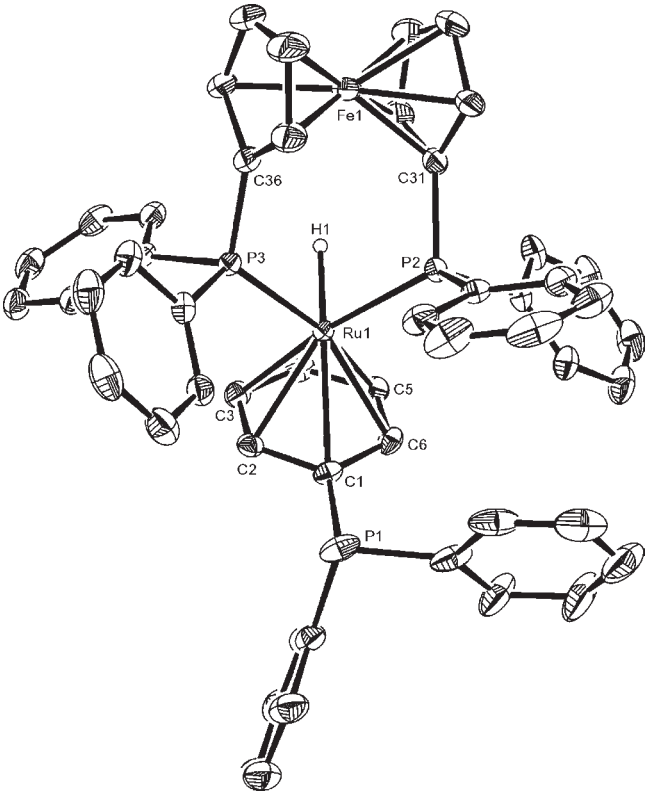

Figure 8. Structure of the cation in [Ru(dppf){(η^6-C_6H_5)PPh_2}H]BAr_4^F (**8**). Thermal ellipsoids are shown at 30% level. All hydrogen atoms, except Ru−H, are omitted for clarity. Selected bond lengths (Å) and angles (deg): Ru(1)−P(2) 2.3001(8), Ru(1)−P(3) 2.3131(8), Ru(1)−C(1) 2.392(3), Ru(1)−C(2) 2.295(3), Ru(1)−C(3) 2.223(3), Ru(1)−C(4) 2.183(3), Ru(1)−C(5) 2.195(3), Ru(1)−C(6) 2.282(3), P(1)−C(1) 1.838(3), P(1)−C(7) 1.827(4), P(1)−C(13) 1.823(4), P(2)−Ru(1)−P(3) 96.03(3).

were observed in the phosphorus spectrum at δ 50.2 and −8.1, with the lower frequency signal assigned to the η^6-coordinated PPh_3 ligand by comparison to the literature.[43] In the $^{13}C\{^1H\}$ NMR spectrum, four low frequency aryl carbon resonances were observed between 94 and 110 ppm arising from the η^6-coordinated ring. The proton NMR spectrum at ambient temperature displayed a single resonance at low frequency at δ −9.32 with a 39 Hz triplet splitting due to the dppf ligand, and somewhat surprisingly, a 7 Hz coupling to the uncoordinated phosphorus center.

Solution Reactivity of 8. The formation of [Ru(dppf)-{(η^6-C_6H_5)PPh_2}H]BAr_4^F (**8**) following chloride abstraction from **1d** presumably reflects the need of the initially formed [Ru(dppf)(PPh_3)H]$^+$ cation to gain electron density. When **8** was treated with either H_2 or N_2, no reaction was observed. Similarly, addition of CO gave very little reaction at room temperature, but upon heating at 343 K for 15 h, the PPh_3 ligand reverted to being P-bound and two molecules of CO were coordinated to give [Ru(dppf)-(PPh_3)$(CO)_2$H]$BAr^F{}_4$ (**9**). The appearance of a single ν_{CO} band in the solution IR spectrum of the compound is suggestive of a trans dicarbonyl geometry, as shown in Scheme 5.[44] This was confirmed by reacting **8** with ^{13}CO,

(40) For an early example of η^6-coordinated PPh_3 ligand see: McConway, J. C.; Skapski, A. C.; Phillips, L.; Young, R. J.; Wilkinson, G. *J. Chem. Soc., Chem. Commun.* **1974**, 327–328.

(41) For other η^6-coordinated group 15 element ligands, see: (a) Becker, E.; Slugovc, C.; Rüba, E.; Standfest-Hauser, C.; Mereiter, K.; Schmid, R.; Kirchner, K. *J. Organomet. Chem.* **2002**, *649*, 55–63. (b) Hermatschweiler, R.; Pregosin, P. S.; Albinati, A.; Rizzato, S. *Inorg. Chim. Acta* **2003**, *354*, 90–93. (c) Caldwell, H.; Isseponi, S.; Pregosin, P. S.; Albinati, A.; Rizzato, S. *J. Organomet. Chem.* **2007**, *692*, 4043–4051.

(42) There are examples of η^6-arene Ru that derive from coordination of BPh_4 anions: (a) Hough, J. J.; Singleton, E. *J. Chem. Soc., Chem. Commun.* **1972**, 371–372. (b) Winter, R. F.; Hornung, F. M. *Inorg. Chem.* **1997**, *36*, 6197–6204.

(43) Pregosin, P. S. *Coord. Chem. Rev.* **2008**, *252*, 2156–2170.

(44) The corresponding chloride complex [Ru(dppf)(PPh_3)$(CO)_2$Cl]BF_4 contains cis-CO ligands. See reference 39.

Scheme 5

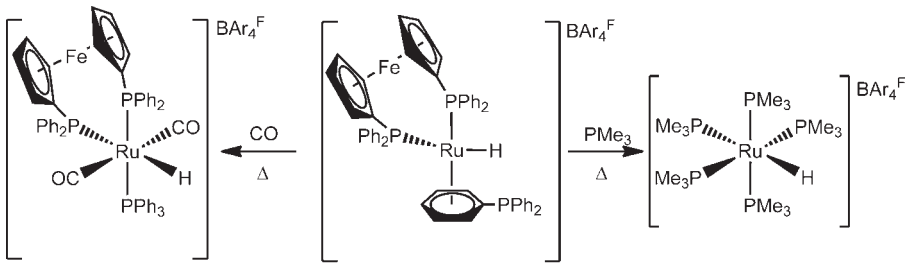

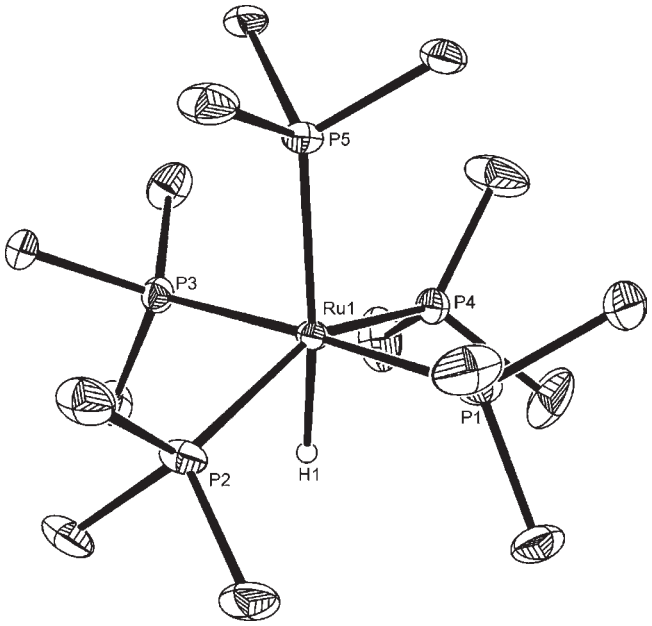

Figure 9. Structure of the cation in $[Ru(PMe_3)_5H]BAr_4^F$ (**10**). Thermal ellipsoids are shown at 30% level. All hydrogen atoms, except Ru−H, are omitted for clarity. Selected bond lengths (Å) and angles (deg): Ru(1)−P(1) 2.3619(12), Ru(1)−P(2) 2.3774(12), Ru(1)−P(3) 2.3653(11), Ru(1)−P(4) 2.3385(13), Ru(1)−P(5) 2.3962(11), P(1)−Ru(1)−P(3) 177.58(4), P(2)−Ru(1)−P(4) 154.02(4), P(1)−Ru(1)−P(5) 91.02(4), P(2)−Ru(1)−P(5) 104.35(4).

which led to the appearance of a triplet hydride signal in the $^1H\{^{31}P\}$ NMR spectrum of **9** at δ −8.56, with a small cis J_{HC} coupling of 5.6 Hz.

Addition of a 5-fold excess of PMe_3 to a THF solution of **8** again generated no new products at room temperature, but upon heating at reflux, afforded two new, highly coupled hydride containing species, which appeared at δ −9.25 and −11.35 in the proton NMR spectrum. After 3 h, the product with the lower frequency resonance was the major product and was assigned as the cationic penta-trimethylphosphine species $[Ru(PMe_3)_5H]BAr^F{}_4$ (**10**, Scheme 5) by comparison with the literature. Although spectroscopic data for **10** has been reported on a number of occasions,[45] we were unable to find either structural or elemental characterization. An X-ray structure determination of the cation in **10** is shown in Figure 9 and reveals a distorted octahedral geometry at the ruthenium center. In particular, of the phosphorus atoms in the equatorial belt of the cation, P2 lies 0.99 Å below the mean plane containing P1, P4, P3, and Ru1.[46]

Conclusions

Treatment of $Ru(PPh_3)_3HCl$ with xantphos, DPEphos, or $(Ph_2PCH_2CH_2)_2O$ affords the corresponding Ru(P−O−P)-$(PPh_3)HCl$ complexes, which have been shown by X-ray crystallography to contain tridentate (i.e., "O in") P−O−P ligands. The cationic aqua complexes $[Ru(P-O-P)(PPh_3)-(H_2O)H]^+$ are formed upon chloride abstraction and readily coordinate small gaseous ligands to yield $[Ru(P-O-P)-(PPh_3)(L)H]^+$ (L = O_2, H_2, N_2), in which the "O in" binding mode is retained. Although the dihydrogen and dinitrogen complexes can only be spectroscopically characterized at low temperature and are far less stable than when L = O_2, metal fragments capable of binding both O_2 and H_2 are relatively rare.[47]

Attempts to mirror this reactivity of the P−O−P complexes with the bidentate phosphine ligand dppf result instead in the formation of the η^6-aryl bound phosphine cation $[Ru(dppf)\{(\eta^6\text{-}C_6H_5)PPh_2\}H]^+$. This shows unexpected reactivity, eliminating both dppf and PPh_3 in favor of a stronger donor ligand such as PMe_3.

Acknowledgment. Financial support was provided by the EPSRC (project studentship for AEWL), a Doctoral Training Award (CEE), and the Swiss National Science Foundation (AM, PSP). Johnson Matthey plc are acknowledged for the kind loan of hydrated ruthenium trichloride. We thank Dr John Lowe for assistance with NMR measurements and simulations and Professor Bob Morris for valuable discussions.

Supporting Information Available: Experimental and simulated ^1H spectra for reaction of **3b** with D_2. CIF files giving X-ray crystallographic data for **1a**−**d**, **2a**, **3a**, **5a**−**b**, **8**, and **10**. X-ray structure of $[Ru(xantphos)(PPh_3)(H_2O)H]OTf$ (CCDC 780098). This material is available free of charge via the Internet at http://pubs.acs.org.

(45) (a) Werner, H.; Werner, R. *J. Organomet. Chem.* **1981**, *209*, C60–C64. (b) Nkosi, B. S.; Colville, N. J.; Albers, M. O.; Gordon, C.; Viney, M. M.; Singleton, E. *J. Organomet. Chem.* **1990**, *386*, 111–119. (c) Burn, M. J.; Bergman, R. G. *J. Organomet. Chem.* **1994**, *472*, 43–54. (d) Holland, A. W.; Bergman, R. G. *J. Am. Chem. Soc.* **2002**, *124*, 14684–14695. (e) Caballero, A.; Carrión, M. C.; Espino, G.; Jalón, F. A.; Manzano, B. R. *Polyhedron* **2004**, *23*, 361–371. (f) Kayaki, Y.; Ikeda, H.; Tsurumaki, J. I.; Shimizu, I.; Yamamoto, A. *Bull. Chem. Soc. Jpn.* **2008**, *81*, 1053–1061. (g) Getty, A. D.; Tai, C.-C.; Linehan, J. C.; Jessop, P. G.; Olmstead, M. M.; Rheingold, A. L. *Organometallics* **2009**, *28*, 5466–5477.

(46) (a) Mathew, N.; Jagirdar, B. R.; Gopalan, R. S.; Kulkarni, G. U. *Organometallics* **2000**, *19*, 4506–4517. (b) Mathew, N.; Jagirdar, B. R.; Ranganathan, A. *Inorg. Chem.* **2003**, *42*, 187–197.

(47) Kubas, G. J. *Metal Dihydrogen and σ-Bond Complexes*; Kluwer/Plenum: New York, 2001.